

## **Reviewing Nearshore Current, Turbidity and Morphology Models**

Colin J.F. Andrews

DSTO-GD-0306

**DISTRIBUTION STATEMENT A**  
Approved for Public Release  
Distribution Unlimited

20020315 176

# Reviewing Nearshore Current, Turbidity and Morphology Models

*Colin J.F. Andrew*

**Maritime Operations Division  
Aeronautical and Maritime Research Laboratory**

DSTO-GD-0306

## ABSTRACT

The aim of this investigation was to review the different types of nearshore current, turbidity, and morphology evolution models currently available and to recommend those most suitable for aiding the planning of amphibious operations. This was achieved by first reading relevant literature and listing the different types of models found within it. Then their relevant attributes (for example: the equations and assumptions utilised in developing them, the parameters needed to utilise them, any validation exercises performed, their findings and their accuracy) were analysed. An important observation made here was that some potentially useful numerical models could not be recommended for usage to the RAN as they required parameters which were too difficult to acquire.

## RELEASE LIMITATION

*Approved for public release*



AQ F02-05-0920

*Published by*

*DSTO Aeronautical and Maritime Research Laboratory  
506 Lorimer St  
Fishermans Bend, Victoria 3207 Australia*

*Telephone: (03) 9626 7000  
Fax: (03) 9626 7999  
© Commonwealth of Australia 2001  
AR-012-071  
November 2001*

**APPROVED FOR PUBLIC RELEASE**

# Reviewing Nearshore Current, Turbidity and Morphology Models

## Executive Summary

There are a number of nearshore characteristics that can have profound effect upon the success of amphibious operations. Such characteristics include wave amplitudes, wave propagation angles, longshore and cross-shore velocities, sand transport rates (an indicator of turbidity) and beach profile characteristics and their temporal changes. Hence, it was envisaged that a set of reports outlining the most appropriate methods (or models) for calculating such parameters would be of great benefit to those planning amphibious operations.

In July 1999, General Document 0214 was produced which reviewed nearshore wave models and made recommendations as to which were suitable to be used. The aim of this investigation was to continue this work and produce a document which outlined the different types of nearshore currents, turbidity, and morphology models. The aim was to then review their attributes (for example: (1) the equations and assumptions utilised, (2) parameters needed to utilise them, (3) any validation exercises performed and their findings) and make recommendations to the Australian Defence Force (ADF) as to which models were most suitable.

An important observation made here was that some potentially useful numerical models could not be recommended for usage to the RAN as they required parameters which were too difficult to acquire.

# Contents

<b>1. INTRODUCTION .....</b>	<b>1</b>
1.1 Stimulus for Report .....	1
1.2 Structure of Report .....	1
1.3 Background Information .....	1
<b>2. LONGSHORE VELOCITY PREDICTIONS.....</b>	<b>9</b>
2.1 Monotonically Sloping Beaches.....	9
2.2 Non-monotonically Sloping (or barred) Beaches. ....	14
2.3 Summary.....	15
2.4 Recommendations.....	15
<b>3. TWO DIMENSIONAL WAVE INDUCED FLOW:.....</b>	<b>16</b>
3.1 Introduction .....	16
3.2 Simple Models of Edge Wave Induced Rips .....	16
3.3 Longshore Bars broken by Regularly Spaced Rip Channels.....	17
3.3.1 Dalrymple (1978) .....	17
3.4 Simple Model of Mega Rips .....	19
3.5 Summary.....	23
3.6 Recommendations.....	24
<b>4. LONGSHORE SEDIMENT TRANSPORT:.....</b>	<b>25</b>
4.1 Introduction .....	25
4.2 Longshore Sediment Transport due to Broken Waves .....	25
4.3 Longshore Sediment Tranport due to Waves and Currents .....	26
4.4 Summary.....	27
<b>5. VERTICAL DISTRIBUTION OF SUSPENDED SEDIMENT .....</b>	<b>28</b>
5.1 Suspended Sediment Concentrations due to Currents:.....	28
5.2 Suspended Sediments Concentrations due to Unbroken Waves: .....	30
5.3 Suspended Sediment Concentration due to Currents and Unbroken Waves .....	30
5.4 Suspended Sediment Concentration under Broken Waves.....	31
5.5 Summary.....	32
5.6 Recommendations.....	32
<b>6. MORPHOLOGICAL MODELLING .....</b>	<b>33</b>
6.1 Spatial Indicative Models.....	33
6.1.1 Summary.....	37
6.1.2 Recommendations .....	37
6.2 Temporal Evolution Models .....	38
6.2.1 Introduction.....	38
6.2.2 Coastal Profile Models .....	38
6.2.3 Coastal Area Models .....	40
6.2.4 Summary.....	40
6.2.5 Recommendations .....	40
<b>7. SUMMARY .....</b>	<b>40</b>

8. SUMMARY TABLE.....	41
9. ACKNOWLEDGMENTS .....	43
10. BIBLIOGRAPHY .....	44
11. PERTINENT LITERATURE .....	48

## 1. Introduction

### 1.1 Stimulus for Report

There are a number of nearshore characteristics that can have profound effect upon the success of amphibious operations, or military operations occurring within the coastal zone. Such characteristics are outlined in Del Balzo, Vodola and Beveridge (1999) and from these those deemed to be of high importance included, wave amplitudes, wave propagation angles, longshore and cross-shore current speeds, sediment transport rates (an indicator of turbidity) and morphology characteristics and changes.

To aid the planning of amphibious operations it was envisaged that it would be beneficial if a set of reports was written outlining the most appropriate methods (or models) for calculating the above parameters.

In June 1999, the first report (namely GD-0214 (Andrew, 1999)) was produced which outlined the most current nearshore wave models and made recommendations as to which were most applicable to the needs of the Australian Defence Force (ADF). This report continues on from where GD-0214 finished and describes those models which forecast those nearshore characteristics described above which were not covered in GD-0124.

This DSTO report, summarising the most appropriate ways of predicting or calculating environmental factors pertinent to amphibious operations, is also important to other DSTO tasks. Most noticeably, the models cited in this report may one day be coded into the Amphibious Warfare Operational Concept System Software (AWOCSS) being developed by Mr Jamie Watson (DSTO Task # 98/165).

### 1.2 Structure of Report

In this report pertinent background information regarding nearshore processes will first be outlined (except background information associated with surface waves; such information was outlined in GD-0214). Then the different types of nearshore models discovered will be summarised, with this report concluding by outlining the most appropriate models for the Australian Defence Force (ADF) based upon the models attributes (assumptions used, parameters required, validation procedures and models accuracy).

**Note:** As in the first literature review (GD-0214), it will be assumed throughout this report that surface wind conditions, deep-water wave characteristics, tidal action, shelf current regimes, and static bathymetry characteristics are readily available for any nearshore forecasting.

### 1.3 Background Information

At some point as a wave propagates towards a coastline, the drag caused by the wave "feeling" the bottom will cause the top stages of the wave to move forward at a greater speed than those at the bottom. At this point the wave will become hydrostatically unstable and break with such a position marking the seaward extent of the surf zone and being strongly dependent upon the depth.

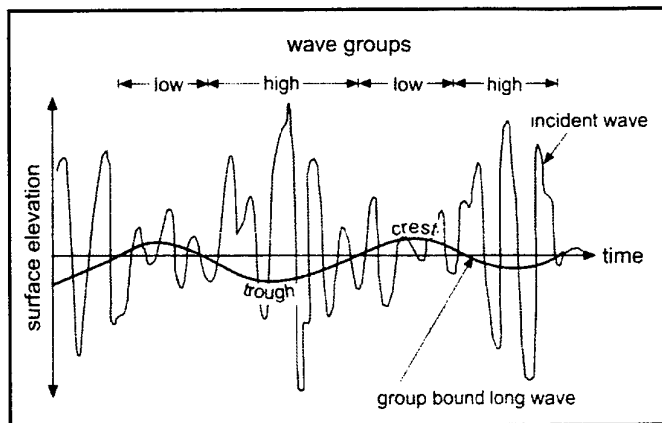
As at any location there is normally a spectrum of wave heights (as well as a spectrum of periods) then due to wave breaking being strongly dependent upon depth, there is a region in which all the waves present will break. This region is part of the surf zone and for obvious reasons is called the breaker zone (Fredsoe and Deigaard, 1992). The seaward extent of the breaker zone is where the waves with the largest height break with the smaller waves breaking further inshore.

When waves break, their momentum is transformed into "plunging", vertical motion, as well as a strong horizontal motion. The momentum flux of this horizontal motion has been given the term radiation stress (Longuet-Higgins and Stewart, 1964) with this body of water having the ability to continue all the way up until it has reached the top stages of the beach face. Here, it is termed swash with the term backwash applied to the swash that runs back down the beach face.

In the surf zone there is a group of waves which are of a very low frequency (0.005Hz - 0.05Hz) and whose presence can influence the formation of longshore currents, rips and longshore bars. These waves are collectively called infragravity waves because of their location in the power spectra of surface gravity waves. However, this collective name is somewhat of a misnomer as they are still gravity waves (Van Rijn, 1998).

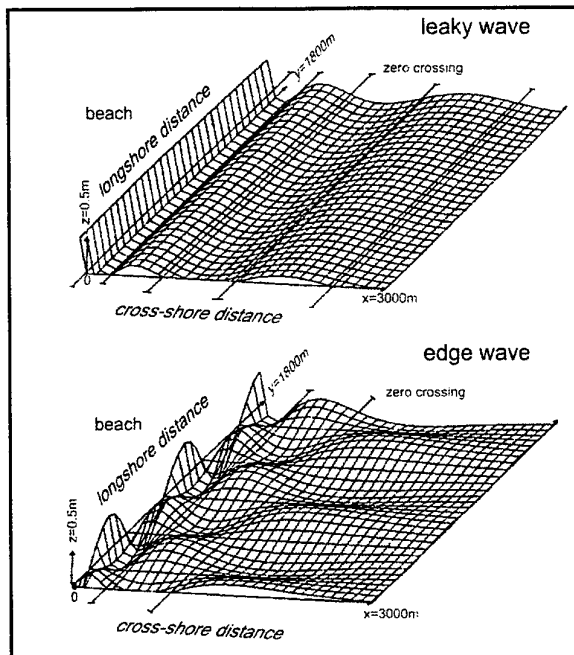
In the ocean there are three types of infragravity waves: Bound Long Waves, Leaky Waves and Edge Waves (Short, 1999). The last two of these are important for the formation of rip currents and multiple sand bars.

Bound Long Waves are associated with the wave packets or wave groups. They are a lowering and increase in the mean water level and arise from the fact that the large waves in a wave group have a higher radiation stress than the smaller waves in the wave groups. Hence, horizontal radiation stress gradients are setup in which it has been theoretically demonstrated by Longuet-Higgins and Stewart (1964) that fluid is expelled from the high waves in the wave groups to the lower waves in the wave groups. This causes a reduction in the mean water level at the position of the large waves and an increase in the mean water level at the position of the lower waves in the wave group. Hence the bound long wave is 180 degrees out of phase with the wave groups (Short, 1999). Figure#1 shows an example of a Bound Long Wave.



Figure#1 A diagram showing the position of a bound long wave with respect to the wave groups. Taken from Short (1999).

Leaky Waves are infragravity waves which have propagated into the surf zone from deeper water but have then been reflected back off the shoreline and back out to sea. Hence energy is "Leaking" out of the surf zone. Their wave height is largest at the shoreline, is constant in the longshore direction and varies in the offshore direction by a succession of alternating maxima and minima of diminishing magnitude (see Figure#2). Leaky waves form when Bound Long Waves approach a beach nearly normally and are released from the wave groups when the short period, incident surface waves break and the wave groupness is destroyed (List, 1992). The released bound long wave then propagates shoreward as a free wave. At the shoreline it is reflected back out to sea with this wave then having the ability to interact with those propagating into the surf zone and thus generate standing leaky waves (Short, 1999).



Figure#2 The surface elevation signature of leaky infragravity waves and edge waves in the surf zone. Taken from Short (1999).

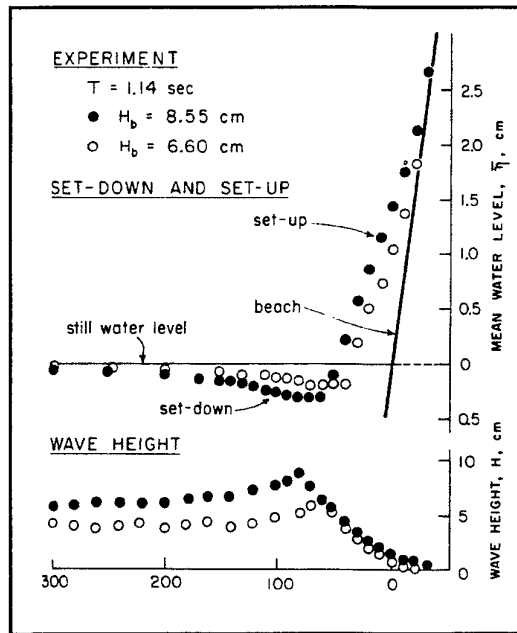
Edge waves are very low frequency waves that travel in the alongshore direction being trapped within the surf zone by depth induced refraction. They have their largest amplitudes at the shoreline, with the amplitude decaying exponentially in the offshore direction and sinusoidally in the longshore direction. Figure#2 shows an example of a simple edge wave. Edge waves of the same frequency, amplitude, and mode but travelling in opposite directions can constructively interfere to produce standing edge waves. Such edge waves are important to the formation of multiple sand bars and have the same frequency as the surface incident gravity waves (Short, 1999).

There are two formation mechanisms for edge waves. For steep, reflective beaches subharmonic edge waves (those having periods twice that of the incident waves) of zero mode are produced by first incident waves being reflected off the shoreline to produce standing waves which, because of a non-linear transfer, are transformed into edge waves. For shallow, dissipative beaches, Gallagher (1971) demonstrated that edge waves could form

as a result of triad non-linear wave to wave interaction in which two obliquely incident bound long waves propagating towards the shoreline could superimpose and generate a third wave (the edge wave) of the same frequency as the incident waves (i.e. synchronous edge waves) with the edge waves not being isolated to zeroth mode (Short, 1999).

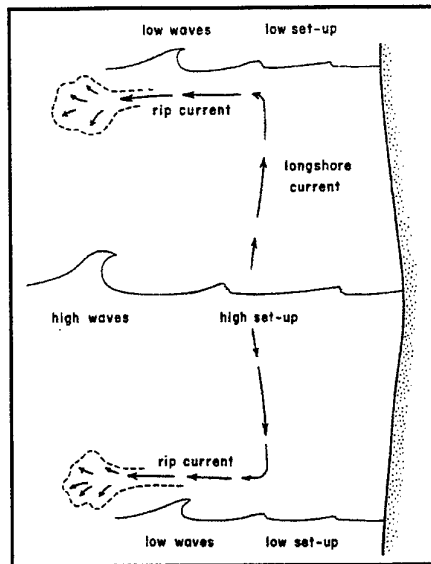
The process of waves approaching a coastline, shoaling, breaking, and running up the beach face is relentless and has the ability to generate longshore velocities between the breaker zone and the swash zone which eventually feed rip currents.

To understand how longshore currents and rips form in the ocean, it first must be understood that the decrease in the onshore radiation stress due to bottom friction is directly balanced by an increase in the wave setup. Figure#3 shows this in detail. It can be deduced from this figure that if there is a longshore variation in the wave setup (caused by a longshore variation in the wave height) then a longshore current is produced in which water will run down the pressure gradient until it converges with other longshore currents generated the same way with the longshore currents then turning seaward and producing rips. Figure#4 shows an example of this scenario.



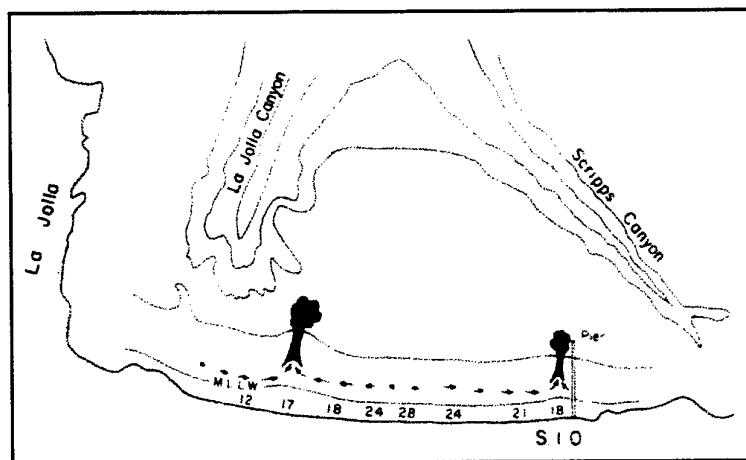
Figure#3 An example of how two waves with different offshore wave heights produce different degrees of wave setup along a shoreline. (Taken from Komar (1998)).

From this analysis it should be deduced that the formation of rip cells is solely related to longshore variations in wave heights. In the ocean wave heights can vary in the longshore direction by two independent mechanisms with each mechanism producing markedly different rip currents. One mechanism is whereby the beach morphology is non-variant in the longshore direction and has edge waves present which are either standing or progressive. As the edge waves have small wave heights which vary sinusoidally along the beach then this causes the surface wave heights and wave setup to vary sinusoidally along the beach. This in turn produces an alongshore pressure gradient which produces longshore currents which flows seaward as rips at the nodes of the edge waves (Komar, 1998).



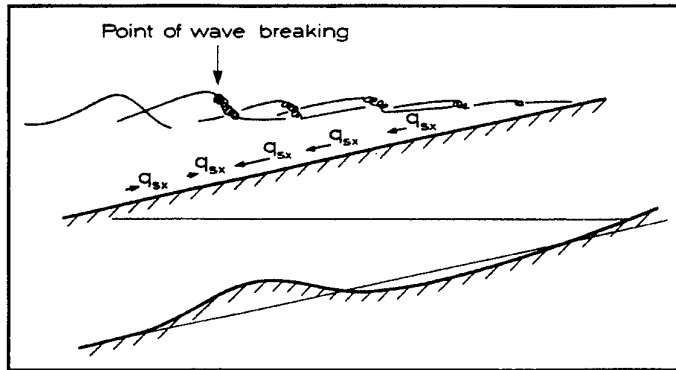
Figure#4 A schematic picture showing how waves of differing heights along a shoreline generate rip currents. Taken from Komar (1998).

The second mechanism is where rips form by wave refraction resulting from bathymetry variations (headlands or offshore canyons or ridges) or wave diffraction due to offshore islands. The wave refraction or diffraction causes wave convergence and divergence zones along the coastline which results in the wave heights to vary in the longshore direction. Like the edge wave formation, this longshore variation in the wave height of the incident waves is translated into a longshore variation in the wave setup which leads to rip formation. Figure#5 shows the location of two permanent rips off California which originate due to the presence off two offshore canyons. For the rips forming as a result of headlands these are called topographic rips and can sometimes be much larger in volume than those caused by the presence of edge waves. Such large topographic rips occur under storm conditions and are called mega-rips (Short, 1999).

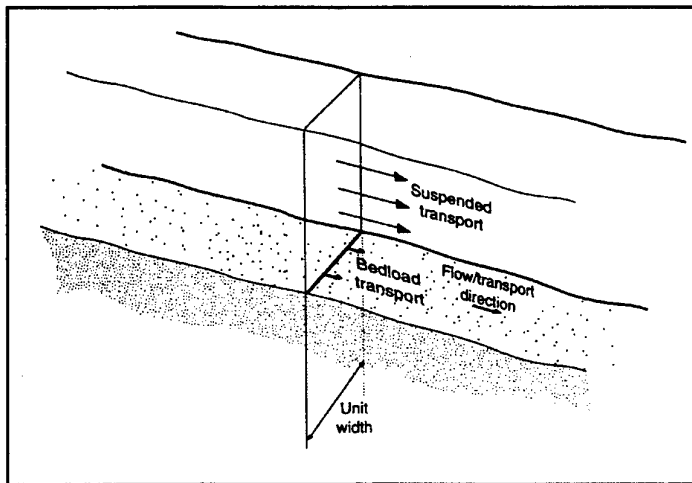


Figure#5 The location of two permanent rips near Scripps Institution of Oceanography (SIO), California, and their close proximity to two offshore canyons. Wave heights along the shoreline are as shown. Taken from Komar (1998).

As far as the beach profile is concerned, erosion first occurs with beach material being placed into suspension by the strong plunging vertical motion accompanying breaking waves. This plunging motion creates an offshore transport over the sea bed which when it converges with the slight onshore transport associated with non-linear (unbroken) surface waves results in the generation of a longshore sand bar (Short, 1999). Figure#6 is a schematic diagram showing such a formation process. Erosion of beach material can then continue as a result of the "wall" of water formed by the breaking waves propagating towards the shoreline and either moving material along the bed (termed bed load transport) and/or by placing more material into suspension (termed suspended load transport). Figure#7 is a schematic diagram illustrating the concept of bed load and suspended sediment load.



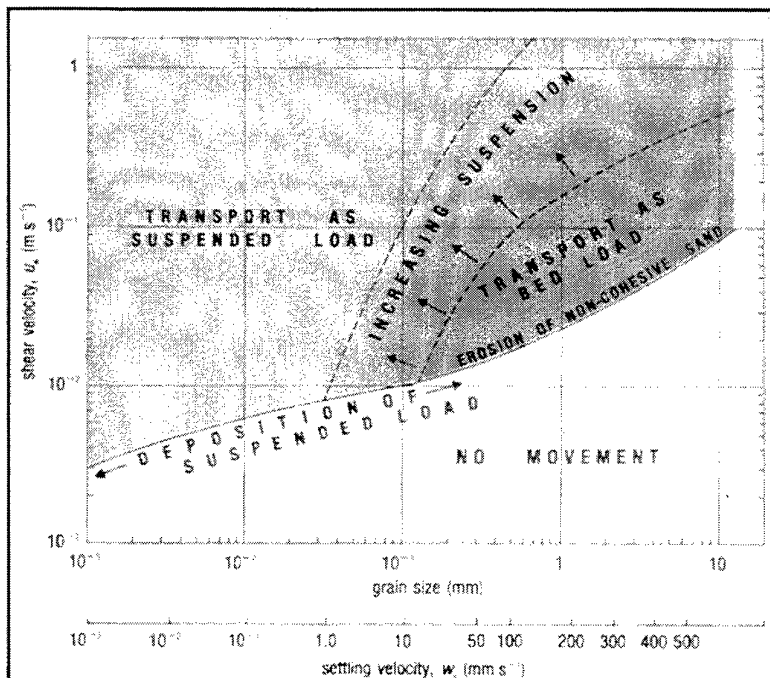
Figure#6 A schematic diagram showing how a longshore bar forms from the convergence of sand transported offshore by breaking waves and the onshore sand transported associated with onshore wave movement.  $q_{sx}$  is the offshore suspended sediment transport rate with arrows lengths indicating relative strengths. (Modified from Fredsoe and Deigaard, 1992)).



Figure#7 A schematic diagram illustrating the difference between bed transport load and suspended transport load. (Taken from Soulsby, 1997).

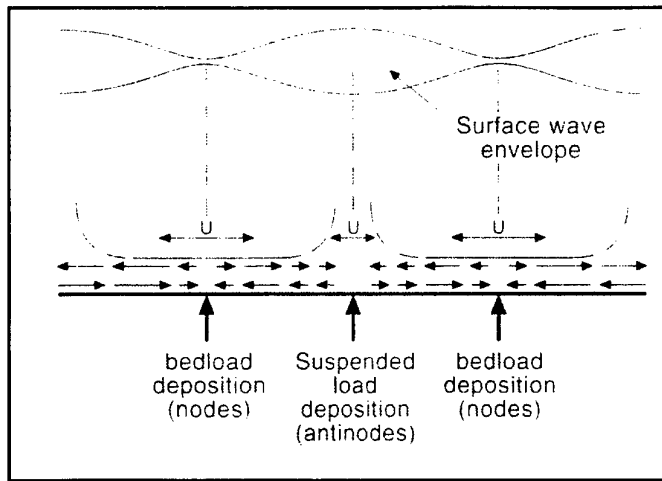
Bed load and suspended load can occur anywhere from the breaker zone to the swash zone, with their magnitudes depending upon the velocity of the broken waves and the particle size distributions of the beach material. Figure#8 shows the dependence of erosion and accretion

upon these two parameters. Bed load magnitudes adjust relatively quickly to changing wave and current conditions: Suspended loads, however, take longer to respond. This is because it takes a finite time and depth for new sediment on the bed to be diffused up through the flow and for sediment in suspension to settle (Soulsby, 1997). Once sand and beach profile material has been placed into suspension, it can then be transported to other locations due to the action of any longshore currents.



Figure#8 The dependence of erosion and deposition of weathered beach sediment upon horizontal velocity and particle sizes. (Taken from Bearman, 1989).

In addition to single longshore sand bars forming as a result of the plunging or vertical nature of broken waves, multiple sand bars can form as a result of standing infragravity waves (edge or leaky) waves. In such a situation the standing edge waves form as a result of the interaction of two progressive edge waves (which may be propagating in the same or in opposite directions) with standing leaky waves caused by the interaction of leaky waves and incoming bound long waves. Such standing infragravity waves induce horizontally segregated drift velocities close to the bed, with the drift converging at the nodes at the bottom of the boundary layers, while the convergence is towards the antinodes somewhat higher in this layer. Figure#9 shows these drift velocity peculiarities for standing infragravity waves. Depending upon whether the mode of sediment transport is by bed load or suspended load will determine where any longshore bars will form. However, as longshore bars form in high energy surf zones, where suspended load dominates, then longshore bars will more often form at the antinodal positions of the standing waves (Short, 1999).

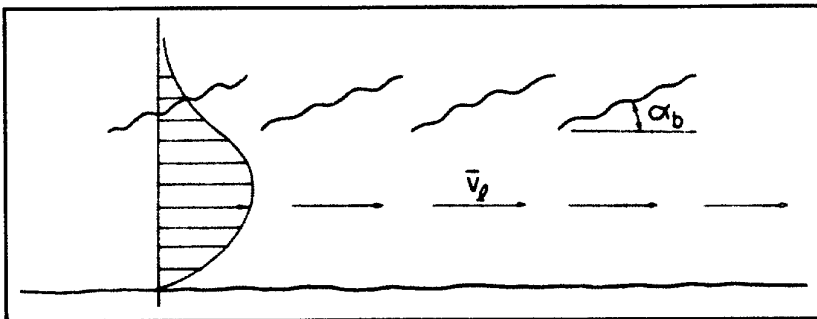


Figure#9 The horizontal velocity ( $u$ ) orbital characteristics beneath a standing infragravity wave and the location of the resulting sand bars when the sediment movement is predominantly in suspended form or in bedload form. Taken from Short (1999).

## 2. Longshore Velocity Predictions

### 2.1 Monotonically Sloping Beaches

The very first models of longshore velocity, caused by obliquely breaking waves on monotonically sloping beaches which had no rips, were proposed by Putman, Munk and Traylor (1949), Inman and Quinn (1951) and Eagleson (1965) (Horikawa, 1988). These models have been reviewed by Galvin (1967) and Komar (1976), and have been largely abandoned (Komar and Oltman-Shay, 1990). Figure#10 shows the circulation scheme which exists under such conditions and shows that the largest longshore velocities occur close to the mid-surfzone position.



Figure#10 A schematic diagram showing the horizontal circulation which forms when waves break obliquely to the shoreline. Adapted from Komar (1998).

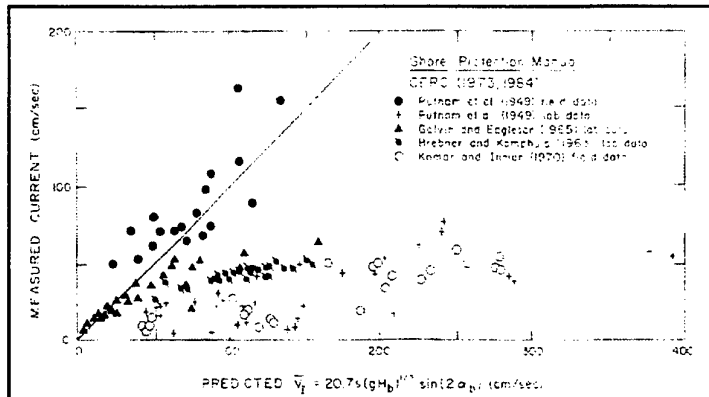
The first meaningful longshore velocity models were simultaneously developed by Longuet-Higgins (1970a,b), Bowen (1969) and Thornton (1970). Such models assumed the waves approaching any beach were monochromatic and stationary in time, that the beach profile had a uniform slope, and that the bottom contours were straight and parallel. To aid obtaining a solution for the longshore velocity these models also assumed that the waves are breaking roughly parallel to the shoreline ( $\cos \alpha_b \approx 1$ ) (where  $\alpha_b$  is the wave approach angle at breaking) and that the maximum velocity of the wave orbitals ( $u_m$ ) are large ( $\sqrt{u_m} < 1$ ) relative to the longshore velocity being predicted ( $v$ ). This last assumption is only valid when ( $\alpha_b < 24^\circ$ ). The major difference in these models was the way in which the horizontal eddy viscosity coefficient was formulated (Komar and Oltman-Shay, 1990).

The model by Longuet-Higgins (1970a,b) (equation#1) was used extensively and was recommended in The Shore Protection Manual (SPM) (CERC, 1984). In supporting their recommendation in the SPM, it was quoted that the model fitted the data by Putnam, Munk and Traylor (1949) and the laboratory data by Galvin and Eagleson (1965). Komar (1998) reviewing this assertion disagreed and reverberated such views using more data sets. Figure#11 shows the comparisons between the equation derived by Longuet-Higgins (1970a,b), the data sets by Putnam, Munk and Traylor (1949) and the Galvin and Eagleson (1965), and other data sets Komar (1998) utilised. It is strongly believed that the discrepancy between the model by Longuet-Higgins (1970a,b) and insitu and laboratory data is the incorporation of the beach slope.

$$v = 0.207 \sqrt{gH_b} \sin(2\alpha_b) \quad (1)$$

where:

1.  $v$  is the longshore velocity ( $\text{ms}^{-1}$ ) at the midsurf position (half way between the shoreline and breakpoint)
2.  $H_b$  is the wave height at breaking.
3.  $S$  is the beach slope.
4.  $g$  is the acceleration due to gravity =  $9.8 \text{ms}^{-2}$ .



Figure#11 A scatter plot showing the model of Longuet-Higgins(1970a,b) and the data sets used to test it. Taken from Komar (1998).

For beaches of constant slope under the action of monochromatic oblique waves the longshore velocity formula developed by Komar and Inman (1970) for the mid surf position provides the best predictions (Komar and Oltman-Shay, 1990). In testing the model by Komar and Inman (1970) on beaches which there were no rips and only longshore velocities, it was observed that equation#2 was applicable up to large breaking angles of 45 degrees and not the ceiling of 24 degrees as inferred by one of the assumptions. The mid surf position is the location where the largest longshore velocities normally occur with the equation developed by Komar and Inman (1970) as follows:

$$v = 0.585 \sqrt{gH_b} \sin(2\alpha_b) \quad (2)$$

where:

1. all the parameters have been previously explained

Recently, a model has been formulated which takes into account that waves are irregular with well defined probability density functions (but which are still assumed to be narrow banded in frequency and direction). The most successful of these (Holman, 1995) was formulated by Thornton and Guza (1986). In this formulation a model is developed by balancing the on-offshore gradient of the wave induced longshore momentum flux (or radiation stress) against the longshore bottom stress and Reynolds stresses. This model assumes that:

- the waves conditions are stationary,

- that the bottom contours are monotonic in the offshore direction (although the model can be extended to non-monotonic beaches by solving the equations iteratively), and are straight and parallel to each other.
- Incident wave angle is small,
- And like the monochromatic wave model of Komar and Inman (1970) assumes that the maximum velocity of the wave orbitals ( $u_m$ ) are large ( $\sqrt{u_m} < 1$ ) relative to the longshore velocity being predicted ( $v$ ).

In applying the above assumptions together with a linear bottom shear stress and Snells law, Thornton and Guza (1983) derived equation#3. This equation is the general solution for beaches of an arbitrary offshore beach profile, although before it can be used equation#4 needs to be solved for  $H_{rms}$  by numerical integration. Thornton and Guza (1983) then simplified equation#3 by considering only beaches which were monotonic in the offshore direction. In doing so they derived an analytical solution for the longshore velocity on-offshore profile (equation#5) with both the analytical model and general beach profile solution only applicable to relatively shallow waters (where the ratio of depth to wavelength is  $< 1/20$ ).

$$v = \frac{3}{4} \frac{B^3 f_p \sqrt{g} \sin \alpha_0 H_{rms}^6}{c_f \gamma^4 C_o h^{9/2}} \quad (3)$$

where:

1. Subscript zero refers to offshore conditions (but the shallow water assumption should still be valid).
2.  $f_p$  is the peak wave frequency.
3.  $\gamma$  is a constant relating the water depth to breaking wave height.
4.  $C_o$  is the wave celerity or phase speed in deep water
5.  $h$  is the water depth.
6.  $C_f$  is the friction coefficient.

$$\frac{d}{dx} \frac{1}{8} \rho g H_{rms}^2 C_g \cos \alpha = \frac{3}{16} \sqrt{\pi} \rho g \frac{B^3}{\gamma^4 h^5} f_p H_{rms}^7 \quad (4)$$

$$v = \frac{23}{20} \frac{g}{\sqrt{\pi}} \frac{a^{1/5}}{c_f} \tan \beta \frac{\sin \alpha_0}{C_o} h^{9/10} \left[ 1 - h^{23/4} \left( \frac{1}{h_o^{23/4}} - \frac{9}{C_o^2} \right) \right]^{-6/5} \quad (5)$$

where:

$$1. \quad a = \frac{23}{15} \sqrt{\left( \frac{g}{\pi} \right) \frac{\gamma^4 \tan \beta}{B^3 f_p}}$$

2.  $B$  is a breaker index parameter and accounts for the different breaker types. This parameter can be visualised as being a function of the amount foam on the face of each bore (Thornton and Guza, 1983) and is expected to be less than unity for spilling breakers and

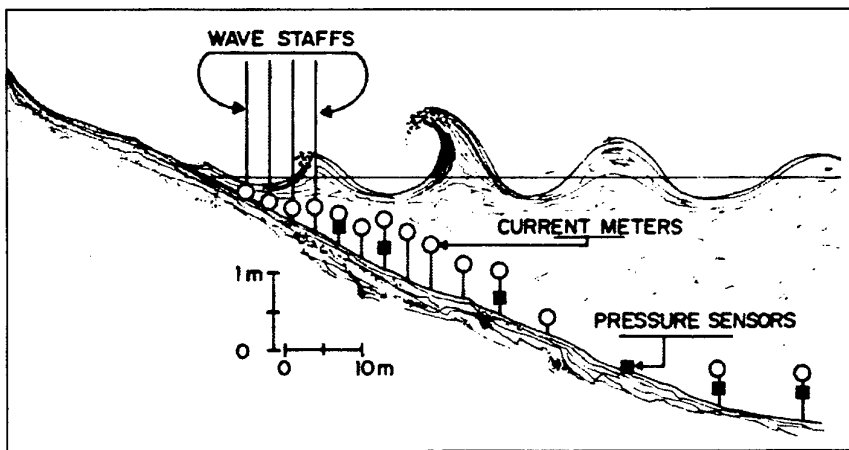
near unity for plunging breakers. Unfortunately this parameters needs to be calculated using insitu wave height data.

The drawback of this analytical model (equation#5) is that too many parameters need to be calculated from *in-situ* data in order for this model to be applied. Such parameters are the

- breaker index B,
- the parameter,  $\gamma$ ,
- offshore wave characteristics of incident wave height, frequency and propagation direction,
- surf zone bathymetry in the offshore direction,
- coastline orientation needs to be calculated using hydrographic data.

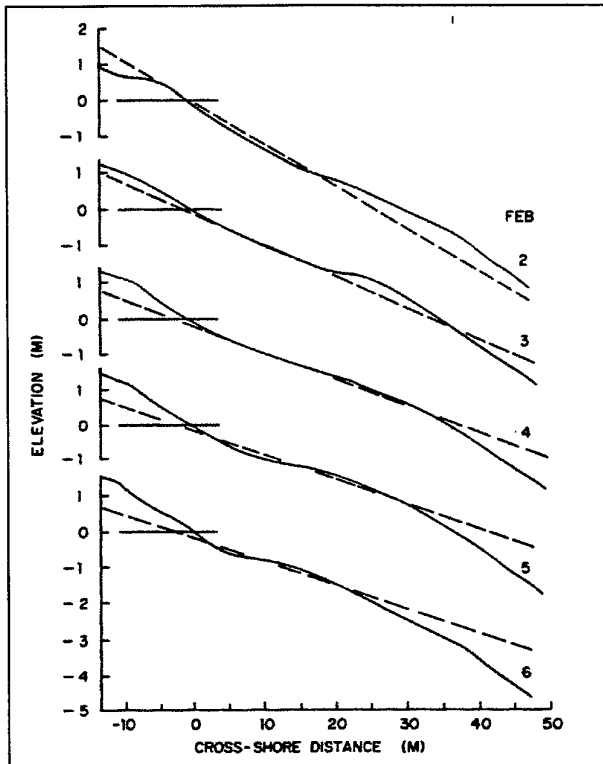
The other drawback from an operational perspective is that the longshore velocity actually needs to be measured at a number of points so that the longshore velocity cross-shore profile can be predicted. The reason for this is that the bottom friction coefficient  $c_f$  cannot be measured *in-situ* and is calculated by measuring the above parameters and then adjusting this coefficient until the difference between longshore velocity predictions and measurements is minimised.

Thornton and Guza (1986) performed such a task using longshore velocity and wave height data collected at Leadbetter Beach, Santa Barbara, California from the 30<sup>th</sup> of January to the 23<sup>rd</sup> of February 1980. This beach was chosen as the wave heights are nearly homogeneous in the longshore direction and the bottom contours are straight and parallel. Although longshore velocity data sets did exist prior to this publication for similar beaches as Leadbetter Beach, their on-offshore instrument spacing was not dense enough (compared to the wavelength) to be useful with the main reason for obtaining this data set was to adequately measure the wave directional properties. Figure#12 shows the position of the instruments in water depth that were greater than 3m.



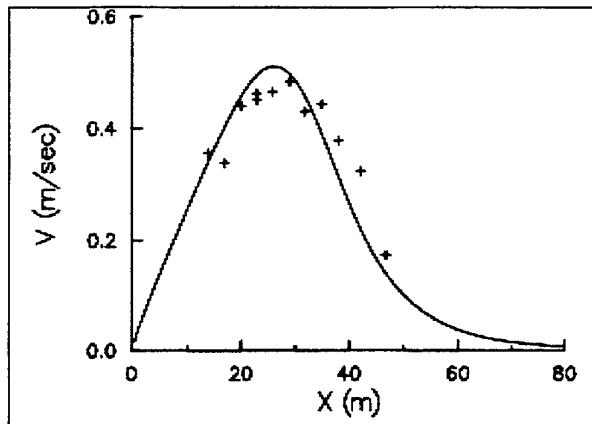
Figure#12 A schematic diagram showing the location of wave and longshore velocity sensors deployed at Leadbetter beach, California between 30<sup>th</sup> January and 23<sup>rd</sup> February 1980. The mean wave period was 14seconds, with the surface elevation of such a wave shown to scale. Taken from Thornton and Guza (1986).

For Leadbetter beach, Thornton and Guza (1986) analysed the data available from the 30<sup>th</sup> of January to the 23<sup>rd</sup> of February 1980 and first restricted themselves to data from the 2<sup>nd</sup> to 6<sup>th</sup> of February. Such a restriction was because this time interval was when the model assumption of narrow banded waves in frequency and direction was valid. During this restricted time interval the model assumption of planar beach offshore profiles was nearly valid and most valid on February 4<sup>th</sup> (see Figure#13).



Figure#13 On-offshore beach profiles and mean profiles of Leadbetter beach from the 2<sup>nd</sup> to 6<sup>th</sup> of February 1980. Note how they are all nearly planar (small single bars) with the most planar profile occurring on the 4<sup>th</sup> of February. Taken from Thornton and Guza (1986).

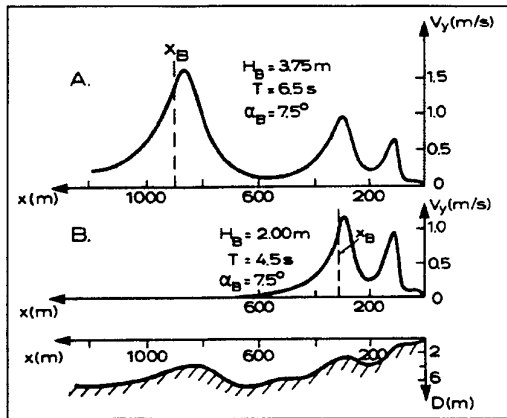
Using offshore and inshore wave characteristics on the 4<sup>th</sup> of February, the wave parameters  $B$  and the parameter  $\gamma$  were calculated. Then the beach orientation was deduced using the orientation of the 50m, 0m, -50m and -100m isobaths referenced to the Mean Sea Level. Lastly, these pieces of information were then used to calculate the cross-shore variation of the longshore velocity by iteratively solving the least square error between the calculated and measured longshore velocities shoreward of the breaker line. This procedure gave the bottom friction coefficient  $c_f$  a value of 0.009. The calculated cross-shore profile and the longshore velocity data used to generate it are as shown in Figure#14. It should be seen from such a figure that the model appears very good, however, such a view can be misleading as to achieve such a comparison the bottom friction coefficient was optimally adjusted. Although a reassuring observation is that the value reached for  $c_f$  was within the range of what has been observed (0.005 to 0.3 (Shemdin *et-al.*, 1978)).



Figure#14 Predicted and measured longshore velocities for Leadbetter Beach, California on February 4<sup>th</sup>, 1980. Taken from Thornton and Guza (1986).

## 2.2 Non-monotonically Sloping (or barred) Beaches.

There have been a few models developed which attempt to estimate the strength of the longshore current on a barred beach. The first of these found in the literature was by Deigaard, Fredsoe and Hedegaard (1986). Although such a model appears very good it does have the common problem of predicting the strongest currents directly over longshore bars and the weakest over the troughs. A characteristic which is inconsistent with detailed



Figure#15 Calculated longshore velocities ( $V_y$ ) for a barred coastal profile for two offshore wave characteristics. Note the location of the maximum velocity over the bar crest although high density data has it located in troughs.  $T$  is the wave period. Taken from Fredsoe and Deigaard (1992).

observations. Figure#15 shows this characteristic.

The best model for predicting the longshore velocity and which goes somewhat to predicting the strongest longshore currents over the troughs is that developed by Smith, Larson and Kraus (1993) (Holman, 1995). This model was developed from that by Larson and Kraus (1991) by including a Turbulent Kinetic Energy term in the radiation stress formulation. Such

an approach shifts the location of the maximum longshore velocities from over the bars shoreward towards the troughs. The model developed improved the agreement between predictions and data by a 20-50% reduction in least squares error (Smith *et-al.*, 1993).

### 2.3 Summary

From critically reading the available literature it was concluded that the best model for calculating the longshore velocity on monotonically sloping beaches of constant slope due to the action of monochromatic oblique waves was developed by Komar and Inman (1970) (as cited by Komar and Oltman-Shay, 1990). If the irregular nature of the wave heights needs to be taken into account then the model by Thornton and Guza (1986) will yield the best results with the model by Smith *et-al.* (1993) (as cited by Holman, 1995) producing the best results for non-monotonically sloping beaches.

### 2.4 Recommendations

By analysing the formulations of the above models and considering what parameters the ADF is likely to be able to measure or predict, the only model which can be recommended is the very basic and least accurate model by Komar and Inman (1970). This is because this is the only model for which all its input parameters (for example surface wave characteristics) can be predicted: The model by Thornton and Guza (1986) would be difficult to implement as bottom friction needs to be measured, with the model by Smith *et-al.* (1993) untenable as turbulent kinetic energy needs to be measured.

### 3. Two Dimensional Wave Induced Flow:

#### 3.1 Introduction

It can be easily stated that no numerical models exist which predict the strength and direction of the horizontal current in the surf zone (which can be decomposed into longshore currents and any rip currents) for arbitrary bathymetry and wave conditions as a function of location as well as time. Such a model would need as input, the time varying surface waves, as well as high resolution bathymetry input of the surf zone and the location of any edge waves as a function of time. The position of edge waves as functions of time is not possible to predict with simply the detection of edge waves very difficult, requiring collecting current data in the energetic surf zone from numerous sensors. Hence models which predict the location and three dimensional structure of any rips do not exist and are unlikely to for at least several years.

What does exist however, is basic quantitative models which permit the

- basic characteristics of rips associated with rip channels (formed by the presence of edge waves) to be quantified.
- longshore spacing of edge wave induced rips,
- formation of mega rips to be predicted,

#### 3.2 Simple Models of Edge Wave Induced Rips

Rips along any beach can be sighted from the air or from the beach by the higher turbidity associated with them compared to neighbouring waters. Rips are also likely to be visually detected in the surf zone by the decrease in the wave height they cause for the incoming waves, as the rip extends seaward out past the breaker zone (Short, 1999). The decrease in the wave height of the incoming waves because of a the rip moving in opposite direction to the waves propagation, is due to the principle of conservation of energy.

The horizontal velocity of a rip as it extends seaward can vary greatly from very low velocities (0.1 to 0.5m/s) to 1 or 2 m/s. The strength of the mean rip velocity is a function of incident wave height as well as the phase of the local tides, with rip velocities increasing under storm conditions and also increasing under low tidal conditions due to the larger wave dissipation over the more exposed longshore bars. Under low tide levels the longshore currents and any rips they feed are also stronger as the flow is constrained to flow in any formed longshore troughs and rip channels. The strength of any rips as they extend seaward has also been observed to pulsate with periods of around 30 seconds to several minutes with this phenomena attributed to far infragravity waves (called shear waves) (Short, 1999).

The longshore spacing between non-topographic rips is approximately four to eight times the surf zone width and depends on the beach slope and wave period; the lower the beach slope the wider the spacing with the spacing also increasing for waves of longer period. On non-sheltered beaches rip spacing can vary from 100m to 500m although commonly rips are 150m to 250m apart (Short, 1999).

If rips form as a result of edge waves, and hence form at the edge wave nodes, then the wavelength of the rips will match that of the edge waves. If the distance between rips needed to be forecasted then the wavelength of the edge waves could be used as a proxy. Unfortunately the detection of edge waves is difficult and time consuming (instrument deployment and data analysis is approximately several days) and needs several longshore or offshore evenly spaced instruments in the vigorous surf zone (for an example see Oltman-Shay (1998)). In terms of predicting the edge wavelength ( $L_e$ ), this is a function of the edge wave period, the beach slope and the edge wave mode, as given in equation#6: Again, parameters which need to be measured. Hence, it would be difficult at the moment for the ADF to forecast the spacing of rip currents. If the spacing between rip currents is important then photographs taken from low flying aircraft would yield the best results.

$$L_e = \frac{g}{2\pi} T_e^2 (2n+1) \tan\beta \quad (6)$$

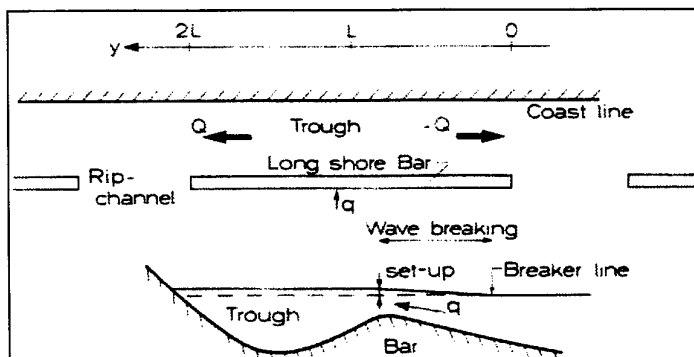
where:

1.  $L_e$  is the wavelength of the synchronous edge wave
2.  $T_e$  is the edge wave period.
3.  $n$  is the edge wave mode number.
4.  $\beta$  is the slope of the surf zone.

### 3.3 Longshore Bars broken by Regularly Spaced Rip Channels

#### 3.3.1 Dalrymple (1978)

The basic model by Dalrymple (1978) was developed to calculate the onshore movement of water ( $q$ ) over a longshore bar and subsequent longshore velocity ( $V$ ) within the trough due to normally incident breaking waves. The bar in this model was of length  $2L$  and was dissected by evenly spaced rip channels. Such rips/rip channels form due to the presence of edge waves (either standing in the longshore direction or progressive). The driving force for the longshore flow in the trough and subsequent offshore flow in the rip channels is longshore variations of wave setup, with such variations being induced by rip channels' effect on wave refraction and because wave breaking in the deeper rip channels is less intensive. Figure#16 is a schematic showing the surf zone geometry of a single bar of length  $2L$  which is bordered by evenly spaced rip channels.



Figure#16 A schematic diagram showing the surf zone geometry of the model developed by Dalrymple (1978). See text for explanation of variables.

The model developed assumes:

- normally incident waves,
- the width of rip channels are large enough so that the longshore flow shoreward of any two neighbouring bars does not interfere,

To determine the magnitude of the onshore current over the bar Dalrymple assumed that the loss in energy was equal to the velocity head of the net discharge over the bar. He also assumed that the bed shear was not important, with later analysis showing that such an approach was justified. The magnitude of the onshore flow ( $q$ ) is given by equation#7a.

$$q = D_c \sqrt{2g(\Delta D_o - \Delta D)} \quad (7a)$$

Where:

1.  $q$  is the onshore flow of water,
2.  $D_c$  is the water depth over the bar crest,
3.  $\Delta D_o$  is the setup when there is no net current and uniform conditions
4.  $\Delta D$  is the actual setup when there is an onshore current.

To calculate the longshore velocity Dalrymple used the longshore projected momentum equation for non-uniform flow as well as the continuity equation. An assumption utilised in this approach was that the wave setup is small compared to the water depth in the trough, which is a valid assumption, and also to neglect bed shear stress. The longshore velocity equation developed is as shown.

$$V = \sqrt{g\Delta D_o} \left( \sinh\left(\frac{\sqrt{2}D_c y}{A}\right) - \tanh\left(\frac{\sqrt{2}D_c L}{A}\right) \cosh\left(\frac{\sqrt{2}D_c y}{A}\right) \right) \quad (7b)$$

Where:

1.  $A$  is the cross-sectional area of the trough.
2.  $\sqrt{g\Delta D_o}$  is simply the gravitational constant multiplied by the wave setup, although will be denoted by the velocity  $V_o$  as it has the same units.

To illustrate an example of using this equation, a longshore bar of 200meters in length was chosen, which had a depth of 1meter at its crest and a trough of area 100m<sup>2</sup> (calculated using the geometry shown in Figure#16). An offshore wave height of 2 meters with a steepness of 1/20 was also chosen. Using the wave steepness, wave height and depth over the bar crest of 1m, Figure#17 from Dalrymple (1978) was used to deduce the magnitude of  $\sqrt{g\Delta D_o}$  (represented as  $V_o$ ) in equation7b, with a value of 1.6m/s reached. Using this value equation7b was then used to calculate the variation of the longshore velocity along the shoreline with Figure#18 generated.

From Figure#18 the longshore symmetry expected in the longshore velocity for a bar dissected by evenly spaced rip channels was observed with the magnitudes predicted in the range one would expect. Although no test could be found for this model the results generated in Figure#18 illustrate that such a model appears very worthwhile.

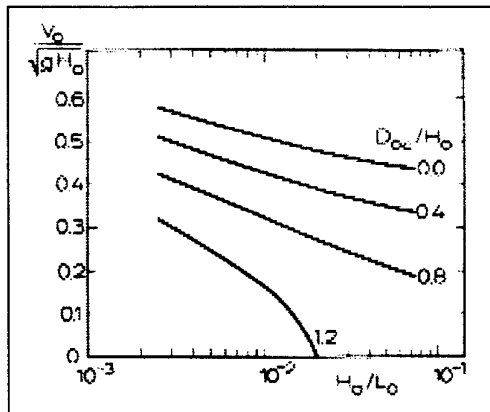


Figure #17 The relationship between the parameter  $\sqrt{g\Delta D_o}$  (defined as  $V_o$ ) as a function of offshore wave steepness ( $H_o/L_o$ ) for differing depths ( $D_{oc}$ ) at the bar crest. Taken from Dalrymple (1978).

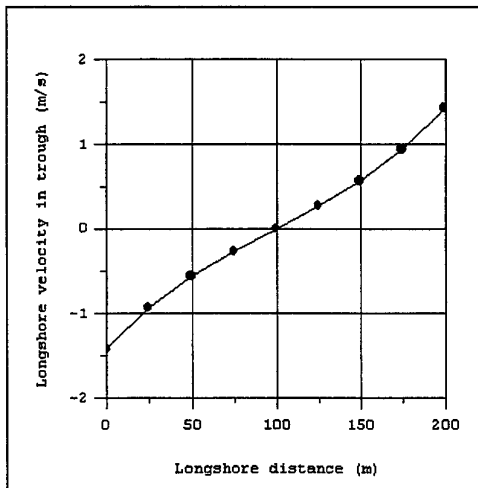


Figure #18 Longshore variation in the longshore velocity in the trough in Figure #16 using Dalrymple's model. See text for beach characteristics.

### 3.4 Simple Model of Mega Rips

In the introduction of this report it was outlined that rips can form due to the presence of headlands (topographic rips), due to the presence of edge waves or due to unique offshore wave refraction schemes. For the first formation scheme, a simple model has been generated which permits the impact headlands have on the cell circulation caused by edge wave rips to be determined. The model, which does not take into account tidal effects, was developed by Martens, Williams and Cowell (1999) and appropriately uses a parameter called the non-dimensional embayment scaling parameter ( $\delta'$ ) (NDESP) (eqn.8). This parameter can be used to predict if topographic rips will form parallel to headlands which are encapsulating an embayment but it should be noted that the NDESP cannot be used to infer if rips will form by edge waves in the interior of embayments.

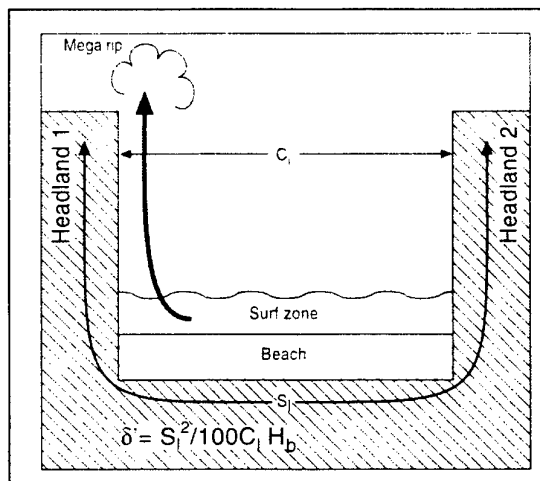
$$\delta' = \frac{S_1^2}{100C_1H_b} \quad (8)$$

where:

1.  $S_1$  is the shoreline length between headlands (see Fig#19).
2.  $C_1$  is the width of the embayment (see Fig#19).

The non-dimensional embayment parameter is a function of the distance between two neighbouring headlands (along the shoreline and also the shortest distance through the surf zone) and also the wave height at breaking. Figure#19 is a schematic diagram showing the parameters used to calculate the non-dimensional embayment parameter. It has been observed that

- topographic rips occur at either end of an embayment when the NDESP is less than 8. Under such conditions the circulation scheme is termed cellular with the coastal dimensions and wave conditions not permitting edge wave rips to form in the interior of the embayment. Under storm conditions topographic rips have stronger velocities, extend further out to sea and are hence termed mega rips.
- embayments have topographic rips and maybe edge wave rips when the NDESP is between 8 and 19. The circulation in this situation is called transitional.
- an embayment will have no topographic rips when the NDESP is greater than 19. It may however have rips forming due to the presence of evenly spaced progressive or standing edge waves. The circulation scheme under this situation is called the normal circulation.



Figure#19 A schematic showing the definition of the parameters used to calculate the non-dimensional scaling parameter. Modified from Short (1999).

In addition to the influence the wave heights and embayment characteristics have on the formation of topographic rips, the beachface slope also has an affect. This is because the beach slope controls the amount of wave energy reflected back out to sea and hence the ability for standing edge waves to form. The more standing edge waves have the ability to form the more a normal rip cell circulation will prevail which will limit the growth of topographic rips.

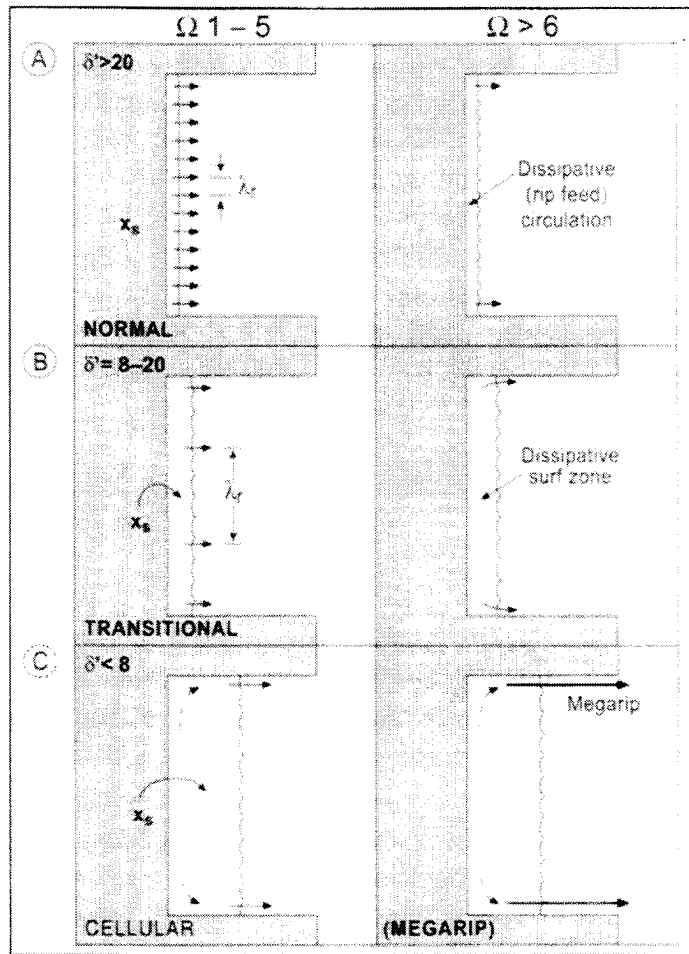
The slope of a beachface cannot be measured once and used for all wave heights and wave periods as it will change with changing wave regimes and is also a function of the sediment making up the beachface. Hence a parameter needed to be developed which allowed the beach slope to qualitatively be predicted knowing the sediment type, wave height and wave period. This parameter is the dimensionless fall velocity (DFV) ( $\Omega$ ) and was developed by Wright and Short (1984) for natural beaches by extending the laboratory work of Gourlay (1968). The DFV is a function of the breaking wave height ( $H_b$ ), wave period (T) and sediment fall velocity ( $\omega_s$ ) (see Eqn#9) and it was observed on natural beaches that when  $\Omega < 1$  beaches were reflective (steep ( $>3^\circ$ ) and with no longshore bars), when  $\Omega > 6$  the beaches were dissipative (flat and with multiple longshore bars), and with beaches being intermediate when  $2 < \Omega < 5$  (with one or two longshore bars).

$$\Omega = \frac{H_b}{\omega_s T} \quad (9)$$

Due to the influence the slope of the beachface has on the rip circulations, Short (1999) extended the work of Martens *et al.* (1999) to illustrate the impact it has on the cell circulations within the surf zone. Figure#20 shows the influence the type of the beach (predicted using  $\Omega$ ) has upon the prevailing cell circulation for steep beaches and for dissipative beaches. It can be seen from this figure that for reflective beaches ( $\Omega = 1-5$ ) with headlands a long way apart ( $\delta' > 20$ ) the rip circulations are solely the result of the edge waves. As the headlands become closer together ( $\delta' < 8$ ) for the same reflective regime ( $\Omega = 1-5$ ) the headlands are too close together to allow edge waves to form. Hence under these conditions the small mass flux of water onto the beach is available to drive topographic rips. For dissipative beaches ( $\Omega > 6$ ), which are beaches for which the ability of edge waves to form diminishes greatly, there is ample mass transport onto beaches to permit topographic rips to form. For such embayments the topographic rips may be present parallel to both headlands or only one depending on the wave approach angles.

In the above paragraphs regarding predicting the formation of topographic rips in embayments, the embaymentisation parameter is a parameter which could be relatively easily calculated by the ADF using topographic charts and wave heights from numerical models. To calculate the dimensionless fall velocity ( $\Omega$ ) however, requires knowledge of the sediment fall velocity  $\omega_s$  which would be difficult to measure in the field by the ADF and as such needs to be calculated.

Initially it was thought that to calculate the settling velocity ( $\omega_s$ ) would, like measuring it, be difficult. By consulting Soulsby (1997) it was observed that the settling velocity is relatively easy to calculate with the best method for calculating it being the formula developed by Soulsby himself (Hallermeier, 1981) (see equation#10a). The advantage of equation#10a is that the only parameter which needs to be guessed (as it would be difficult to measure) is the median grain size (d). Such a parameter can be guessed by taking a sample of the sediment and visually analysing it for content. The other parameters of the settling velocity which can be taken as constant are the grain and sea water density ratios (s) and the kinematic viscosity of sea water (V):



Figure#20 A schematic showing the rip circulation schemes which form as a function of the dimensionless embayment parameter and the beach type (depicted by the dimensionless fall velocity ( $\Omega$ )). Taken from Short (1999).

- the density ratio of sea water to sediment can be taken as a constant as it can be assumed beaches are composed of sand ( $\rho_s = 2650 \text{ kgm}^{-3}$ ) and that the sea water density can be a constant  $1027 \text{ kgm}^{-3}$ . Hence (s) in equation#10b can be taken as 2.58 (dimensionless).
- The kinematic viscosity changes so little (see Figure#21) that it can be taken as  $10^{-6} \text{ m}^2\text{s}^{-1}$ , although it can be accurately calculated knowing the temperature of the sea water and is such a small function of salinity that including salinity in the calculations is deemed not necessary. Figure#21 shows the dependence of the kinematic viscosity on the water temperature for fresh water (zero salinity) and for a salinity of 35psu (practical salinity units).

$$\omega_s = \frac{v}{d} \left[ \sqrt{(10.36^2 + 1.049D_s^3)} - 10.36 \right] \quad (10a)$$

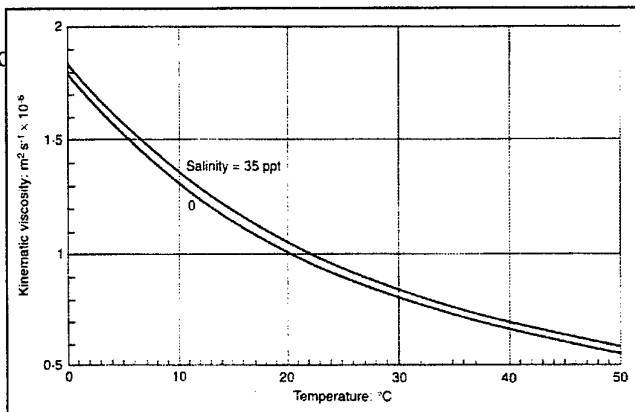
where:

1.  $\nu$  is the kinematic viscosity of the sea water
2.  $d$  is the median diameter of the sediment
3.  $D_*$  is the dimensionless grain size and given by equation#10b

$$D_* = d \left[ \frac{g(s-1)}{\nu^2} \right]^{\frac{1}{3}} \quad (10b)$$

where:

1.  $s$  is the ratio of specific gravity



Figure#21 The dependence of kinematic viscosity on temperature for freshwater (zero salinity) and a salinity of 35ppt (parts per thousand). Taken from Soulsby (1997).

From the above paragraphs, it was concluded that the model by Martens *et-al.* (1999), enabling the presence of topographic rips to be predicted, is a relatively simple model to apply and would be a valuable tool for the ADF. The two components of this model, namely the embayment parameter and the dimensionless fall velocity, are also relatively simple to calculate with all that is needed being topographic charts and wave heights for the embayment parameter, and sediment characteristics for the dimensionless fall velocity.

### 3.5 Summary

From reading the available literature it is concluded that there are no numerical forecasting models available which can predict the strength of the horizontal current in the surf zone due to gradients in the radiation stress as a function of time and location and that such a model is unlikely to be available for a long time (more than 5 years). What has been shown are the magnitudes of basic rip characteristics (velocities and longshore spacings), as well as models which;

- predict the longshore spacing of rips caused by the presence of edge waves,
- predict the rip characteristics for longshore bars which are evenly dissected by rip channels
- predict the ability of topographic rips to form in embayments.

### 3.6 Recommendations

From reading the relevant scientific literature it can be stated that the broad scale characteristics of rips (their strengths and longshore spacings) are known and that such values can be used by the ADF. The scientific literature also yielded numerical models of rip characteristics, as well as their feeder currents. By comparing the input required by these models with the capabilities of the ADF it was concluded that the models which can be recommended to the ADF include:

- The model by Dalrymple (1978), which permits the longshore velocity longshore variation behind a single bar, which is evenly dissected by rip channels.
- The model by Martens *et-al.* (1999) which permits the formation of topographic rips in embayments to be predicted.

## 4. Longshore Sediment Transport:

### 4.1 Introduction

For military operations knowing the visibility of the water column at any depth is a very worthwhile parameter to be able to forecast. Such a parameter, for example, is helpful to clearance divers conducting mine warfare operations. One parameter of visibility is the amount of sediment within the water column. In Section#5 of this General Document, models which permit the sediment concentrations as a function of depth to be predicted will be outlined. However, before this takes place it was considered that as a precursor, models which permit the total longshore sediment transport to be predicted within the surf zone due to the action of breaking waves (or longshore radiations stress gradients) should be outlined. Such models are not directly applicable to any facet of military operations and have been summarised here only for completeness.

### 4.2 Longshore Sediment Transport due to Broken Waves

One of the most widely used methods for calculating the total longshore sand transport (non-cohesive sediment) across the surf zone was developed by CERC (Coastal Engineering Research Centre) (Soulsby, 1997). This formula, however, can only be applied to beaches with the following characteristics:

1. Fine to medium sediment grain sizes (diameter < 0.5mm)
2. Beaches with no tidal currents (thus inhibiting its applicability to the northern Australian coastal zone).
3. Low beach slope < 1:100
4. Straight beaches

The CERC formula has been superseded by the Queens formula (<http://www.ihe.nl/he/dicea/sed41/sed4102.htm>). This is because Schoones (1996) comparisons of the Queens formula and others against *in-situ* data revealed that it is the best currently available (Holman, 1995). Schoonees also highlighted the fact that the Queens formula is a lot more applicable than the CERC formula.

The Queens formula was derived from dimensional analysis and is expressed as follows.

$$Q = \frac{KH^3\rho}{T} \left( \frac{H_b}{L_o} \right)^{1.25} (\tan \beta)^{0.75} \left( \frac{H_b}{d_{50}} \right)^{0.25} (\sin 2\alpha_b)^{0.6} \quad (11)$$

Where:

- (1) Q is the longshore sand transport rate in Kg/s
- (2) K is a dimensionless constant which can be determined from field data, although Kamphuis (1986, 1990), using an extensive data set, observed a value of  $1.3 \times 10^{-3}$ .
- (3) is the sea water density
- (4) H is the mean water depth
- (5) T is the peak period of the spectrum of waves

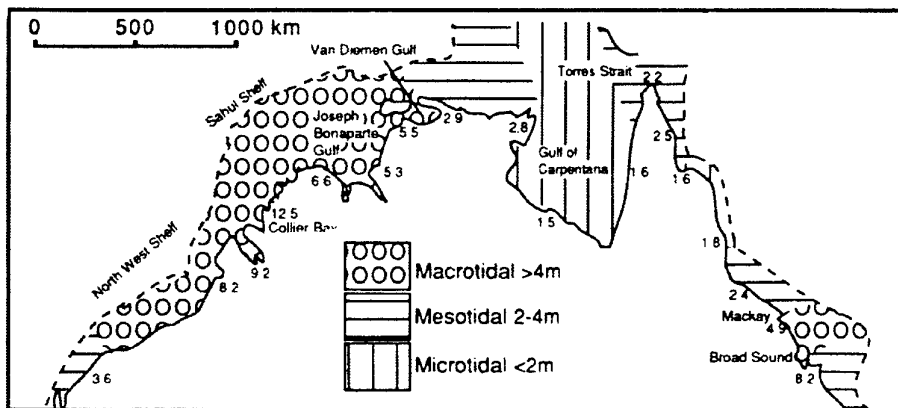
(6)  $d_{50}$  is the median grain size

Despite the success the Queens formula has had, it still has inherited restrictions. Similar to the CERC formula, the Queens formula should only be applied to beaches with the following characteristics:

1. no tidal currents (which, like the CERC formula, inhibits its applicability to the northern Australian coastline).
2. straight beaches with no groynes or breakwaters.
3. plane (monotonically) sloping beaches with no longshore bars.

### 4.3 Longshore Sediment Transport due to Waves and Currents

As specified above, the CERC and Queens formulas should only be applied to beaches where the horizontal speed of any external currents (ie Ekman, tidal, geostrophic) is very low (typically < 20% of the longshore velocity induced by waves) Soulsby (1997). Hence, for the strong tidal regimes of the northern Australian coastline (see Fig#22) other formulations needed to be found.



Figure#22 The tidal regimes encountered around the Australian coastline. Note how the northern Australian coastline has large tidal fluctuations. Modified from Harris (1994).

From Soulsby (1997), four models are described for nearshore environments which may have strong external currents. The first was by Bailard (1981) and was developed using the "energetics" arguments of Bagnold, Inman and Bowen. Such an argument can be summarised as saying that the work done in transporting sediment is a fixed proportion of the total energy dissipated by the flow.

The model formulated by Bailard was for bed and suspended load and can include the effects of wave asymmetry and bed slopes. Applying the model however, to surf zones with rippled seabeds can result in unrealistic sediment transport predictions with the model also only being applicable when low external currents exist.

For bed and suspended load over rippled beds, the models by Soulsby-Van Rijn (see Soulsby (1997) page 183) or Van Rijn (1989) should be used. The model by Soulsby was developed by applying the principles of Grass (1981) to the current induced transport model by Van Rijn

(1984) and modifying it to include a sediment threshold term and a bed slope term (Souslsby, 1997). The model Van Rijn (1989) was developed by adapting his current alone formula (namely Van Rijn (1984)) to include an analytical, semi-empirical, model of sediment diffusion through the wave boundary layer. It is quite a complicated model and calculates both longshore velocities as well as suspended loads and bed loads. Comparisons of the model results with *in-situ* data are quite good (Souslsby, 1997).

The fourth model is the Sediment Transport at a Point model (STP) and like the Van Rijn model is an extensive computer based model which calculates longshore velocities as well as longshore sediment transports. It can be purchased from the Danish Hydraulic Institute and has the advantage of being updated regularly with new processes and features. In this model coastal beds can be rippled or nonrippled, graded or of uniform material and surface waves can be breaking or non-breaking with these types of models classified as being the "best way forward in developing more advanced, accurate, reliable sediment transport prediction methods" (Souslsby, 1997).

An interesting observation of these types of models was made by Deigaard (1998). He observed that they are comparable to much simpler models (namely the Bailard formula). Hence it is thought that the more complex models could be used to calibrate the simpler models, which have the major advantage of not needing so much computing resources.

#### 4.4 Summary

From critically reading the available literature it has been concluded that the best simple model for calculating the longshore sediment transport rate (or the vertically integrated sediment concentration multiplied by longshore velocity) in the nearshore (where the waves have broken) is the Queens formula (Holman, 1995) with the model by Bailard (1981) used for non-rippled beaches where strong external currents exist. For rippled beds the models by Souslsby or Van Rijn should be used. Finally, the computer intensive STP (Sediment Transport at a Point) model by the Danish Hydraulic Institute is recommended for calculating the sediment transport over a grid and can be applied to rippled or non-rippled beds and accounts for broken as well as unbroken waves. This model, however, is expensive to purchase.

## 5. Vertical Distribution of Suspended Sediment

The vertical distribution of sediment concentration in the water column within and seaward of the surf zone is an important parameter in predicting the underwater visibility. By knowing the visibility range, well informed decisions can then be made as to how the detection of objects within the nearshore can proceed.

### 5.1 Suspended Sediment Concentrations due to Currents:

Due to the large tidal amplitudes which occur along the northern Australian coastline (see Fig#22) it was envisaged that there may be occasions when strong tidal velocities exist in the absence of any significant waves. Hence, it was thought that some time should be taken to outline those models which calculate the vertical suspended sediment concentration arising solely as a result of currents.

In the sea, the model which appears to correspond best to data is that developed by Van Rijn (Soulsby, 1997). This model was based upon the steady state balance between the settling of sediment due to gravity and the upward diffusion resulting from turbulence. This balance can be expressed by equation#12, with Van Rijn making the assumption that the turbulent diffusivity of sediment varies parabolically in the lower half of the column and is constant in the upper half. The model by Van Rijn can be applied to regions which do, or do not have, rippled beds.

$$\omega_s C(z) = -K_s \frac{dC(z)}{dz} \quad (12)$$

where:

1.  $C(z)$  is the suspended sediment concentration at a height  $z$  above the bottom,
2.  $K_s$  is the turbulent diffusivity of sediment.

#### Van Rijn Model:

$$\boxed{\begin{aligned} C(z) &= C_a \left[ \frac{z}{z_a} \cdot \frac{(H - z_a)}{(H - z)} \right]^{-b} && \text{for } z_a < z < \frac{H}{2} \\ C(z) &= C_a \left[ \frac{z_a}{H - z_a} \right]^b \exp \left[ -4b \left( \frac{z}{H} - \frac{1}{2} \right) \right] && \text{for } \frac{H}{2} < z, H \end{aligned}} \quad (13)$$

With

$$b' = \frac{b}{B_1} + B_2$$

$$B_1 = 1 + 2 \left( \frac{\omega_s}{u_*} \right)^2 \quad \text{for } 0.1 < \frac{\omega_s}{u_*} < 1$$

$$B_1 = 2 \quad \text{for } \frac{\omega_s}{u_*} \geq 1 \quad (13b)$$

$$B_2 = 2.5 \left( \frac{\omega_s}{u_*} \right)^{0.8} \left( \frac{C_a}{0.65} \right)^{0.4} \quad \text{for } 0.01 < \frac{\omega_s}{u_*} < 1$$

$$B_2 = 2 \quad \text{for } \omega_s > u_* \text{ or } z_a > 0.1H \quad (13c)$$

where:

1.  $z_a$  is a reference height near the seabed,
2.  $C_a$  sediment reference concentration at the height  $z_a$
3.  $H$  is the water depth
4.  $b$  is the Rouse number ( $\frac{\omega_s}{0.40u_*}$ ) or suspension parameter ( Soulsby, 1997)
5.  $u_*$  is the friction velocity ( $\sqrt{\frac{\tau}{\rho}}$ ) where  $\tau$  is the vertical stress and  $\rho$  is the water-sediment mixture density.

The reference concentration  $C_a$  and the reference height  $z_a$  at which it is calculated must both be evaluated before the model can be employed. Several formulae have been developed with Garcia and Parker (1991) testing seven and recommending the following two:

Smith and McLean (1977):

$$C_a = \frac{0.00156 T_s}{1 + 0.0024 T_s} \quad (13d) \text{ at a height}$$

$$z_a = \frac{26.3 \tau_{cr} T_s}{\rho g (s-1)} + \frac{d_{50}}{12} \quad (13e)$$

where:

$$(1) \quad T_s = \left( \frac{\tau_{os} - \tau_{cr}}{\tau_{cr}} \right)$$

(2)  $\tau_{os}$  is the skin friction bed shear stress

(3)  $\tau_{cr}$  is the threshold bed shear stress to initiate sediment movement

Van Rijn (1984)

$$C_a = \frac{0.015 d T_s^{3/2}}{z_a D_*^{0.3}} \quad (14) \text{ at a height}$$

$$z_a = \frac{\Delta_s}{2} \quad (14b)$$

Where

(1)  $\Delta_s$  is the height of sand bed waves (see page 116 of Soulsby (1996) for formulations)

(2)  $D_*$  is the dimensional grain size =  $\left[ \frac{g(s-1)}{v^2} \right]^{1/3} d_{50}$  (see section 3.4 for an evaluation method).

## 5.2 Suspended Sediments Concentrations due to Unbroken Waves:

In nearshore regions seaward of the breaker zone the suspended sediment resulting from wave induced turbulence is largely confined to the relatively thin (few cm's or mm's) bottom boundary layer. As this thickness is too small to be of importance to divers or robotic vehicles, this section has been included for purely academic reasons.

For rippled seabeds the turbulent sediment diffusivity is assumed constant with height and the concentration profile is given by the following equation:

$$C(z) = C_0 \exp(-z/l) \quad (15)$$

Where:

1.  $C_0$  is a reference concentration at the seabed ( $z=0$ )
2.  $l$  is a sediment concentration decay length scale,

For  $C_0$  and  $l$ , various expressions have been developed, of which the most widely accepted formulae are those developed by Nielsen (1992) (Soulsby, 1997) (see page 145 of Soulsby (1997) for a complete description).

As the above equation was developed for rippled seabeds (as would be expected in the presence of surface waves) then it should come as no surprise that it should not be used for sheet flow (flat-bed) conditions. In such situations a better expression to use is analogues to a formula which is sometimes used for determining suspended sediment concentrations due to currents over flat beds. The formula is as follows:

$$C(z) = C_a \left( \frac{z}{z_a} \right)^{-b} \quad (16)$$

Where:

1.  $b$  is a constant dependent upon the median grain diameter.

## 5.3 Suspended Sediment Concentration due to Currents and Unbroken Waves

The suspended sediment concentration due to waves and currents first originates in the wave boundary layer and then diffuses upward through the water column as a result of the turbulence of the current. Both of these processes are effected by the interaction of the wave boundary layer and the current boundary layer, with the concentration profiles, although not being well established, typically described for flat beds by the following formulae (Soulsby, 1997).

$$C(z) = C_a \left( \frac{z}{z_a} \right)^{-b_{max}} \quad \text{for } z_a \leq z \leq z_w \quad (17)$$

$$C(z) = C(z_w) \left( \frac{z}{z_a} \right)^{-b_m} \quad \text{for } z_w \leq z \leq h \quad (18)$$

Where:

$$1. \quad b_{max} = \frac{\omega_s}{0.40u_{*max}}$$

$$2. \quad b_m = \frac{\omega_s}{0.40u_{*m}}$$

$$3. \quad z_w \text{ is the wave boundary layer thickness} = \frac{u_{*max} T}{2\pi}$$

$$4. \quad u_{*m} = \sqrt{\left( \frac{\tau_m}{\rho} \right)} \text{ and } u_{*max} = \sqrt{\left( \frac{\tau_{max}}{\rho} \right)}$$

5.  $\tau_{max}$  is the maximum bed shear stress in one wave cycle

6.  $\tau_m$  is the mean bed shear stress in one wave cycle

7.  $C_a$  can be calculated using either the Van Rijn (1984) formula or the Smith and McLean (1977) formula outlined above.

Meanwhile, if the concentration profile  $C(z)$  is required above a rippled seabed, then the above model can still be applied, although skin-friction values of and should be used in the calculation of the reference concentration and total stress values should be used to calculate  $b_m$  and  $b_{max}$ .

All of the above formulations for the suspended sediment profile are empirically based with each based upon a particular set of assumptions. The most advanced method for calculating the suspended sediment concentrations (as well as transport rates) is by means of a numerical model of the wave plus current boundary layer, utilising some form of turbulent energy closure scheme. The Danish STP model is one such model of this type and was reported above for longshore sediment transport. It has an advantage that it can be applied to plane as well as rippled beds (Soulsby, 1997).

#### 5.4 Suspended Sediment Concentration under Broken Waves

Waves are rarely monochromatic with a spectrum of wave frequencies and heights normally occurring. As waves normally break along any shoreline as a function of depth, there is a horizontal distance between where the first waves break and where all waves have broken. Such a region is called the "outer zone" of the surf zone (see Fig#23) (Fredsoe and Deigaard, 1992), with the complexity of the turbulent kinetic energy associated with breaking of waves in this region not sufficiently known to permit the suspended sediment concentrations to be predicted (Fredsoe and Deigaard, 1992).

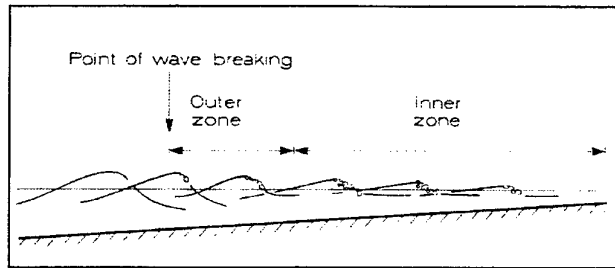


Figure #23 A schematic diagram showing how the surf zone can be dissected into an outer zone (where wave breaking occurs) and an inner zone (where all broken waves have organised themselves as hydraulic bores). Taken from Fredsoe and Deigaard (1992).

In the inner zone, however, where the broken waves have arranged themselves as hydraulic bores, the effect of the turbulence upon the suspended sediment concentration can be described by using the turbulent viscosity formulation:

$$v_T = l\sqrt{k} \quad (19)$$

where:

1.  $l$  is the length scale of the turbulence (see page 166 of Fredsoe and Deigaard (1992) for more information (and equations)).
2.  $k$  is the turbulent kinetic energy.

The turbulent viscosity formulation can then be placed into the sediment continuity equation which is then solved numerically to obtain the suspended sediment concentration (Fredsoe and Deigaard, 1992).

## 5.5 Summary

For forecasting the sediment concentration profile in the vertical (which is very helpful in forecasting the horizontal visibility range) due solely to the action of horizontal currents the model by Van Rijn is recommended and it can be applied to regions which do, or do not have, rippled beds. The sediment concentration in the vertical due to the action of currents and unbroken waves is easily modelled by assuming that the concentration is linearly varied. The sediment concentration due to broken waves can only be forecasted in the inner surf zone. This is because it is only here that the broken waves have arranged themselves as hydraulic bores with the effect of the turbulence upon the suspended sediment concentration described by the turbulent viscosity formulation in equation #19.

## 5.6 Recommendations

Although numerical models are available which predict the concentration of sediment in the vertical under a wide variety of environmental conditions, by analysing such models it should quickly be seen that it would be difficult to apply them in an operational sense by the ADF. The reason is that virtually all the models specified above require a lot of *in-situ* data which would require new skills to be learnt by ADF personnel and considerable man hours expended in gathering and analysing the necessary *in-situ* data. Hence, none of the above models can be recommended for usage.

## 6. Morphological Modelling

In this section, models which allow the broad scale cross-shore characteristics of the beach morphology to be predicted are examined using Short (1999). Also examined are models that predict how such characteristics vary in time. These temporal models have been included in this report for two reasons. First, they permit the determination of how the topography has changed due to storms. Secondly, they permit the evolution of the bottom topography (due to changes in wave, tide, wind and current conditions) to be described over longer time scales (for example monthly and seasonal).

### 6.1 Spatial Indicative Models

From reading the current literature it was concluded that there are currently no numerical models in existence which permit the two dimensional (longshore and cross-shore) morphology of the surf zone to be predicted. There are models which allow the user to observe what morphology will result when different combinations of edge waves exist (for example Holman and Bowen (1982)), but such models are usually used to determine which combinations of edge wave modes must be present in the surf zone to form a particular type of morphology. Such models cannot be used in a predictive or operational mode.

There are models however, which indicate the cross-shore characteristics of morphology, such as the number of longshore bars, where the bars are located and the spacing between any rip channels, and these are outlined extensively in Short (1999). Also outlined in Short (1999) are empirical formulations to predict the slope of the beachface.

Predicting which beaches will have longshore bars and also predicting how many bars will exist parallel to any beach has been addressed by several authors with Short and Aagaard (1993) reviewing them and using field data from microtidal sandy beaches to introduce a new bar parameter ( $B_*$ ). This parameter assumes that:

- existence of any longshore bars is due to the existence of a dominant cross-shore standing infragravity wave.
- cross shore profile can be approximated by a linear slope  $\tan(\beta)$  which terminates at a constant depth at a distance of  $x_s$  from the shoreline.
- infragravity wave period is directly proportional to the incident wave period.

The equation of this parameter is outlined below with the magnitude of it versus the number of bars outlined in table #1.

$$B_* = \frac{x_s}{gT^2 \tan \beta} \quad (20) \quad (\text{Short and Aagaard, 1993}).$$

where:

1.  $T$  is the incident wave period and used as a surrogate for the infragravity wave period.

Table#1 The number of bars which correspond to the magnitudes of  $B_s$ . Taken from Short (1999).

$B_s$	<20	20-50	50-100	100-400	> 400
Number of bars	0	1	2	3	4

For longshore bars which have formed due to the presence of standing infragravity waves the location of the sand bars crests or troughs in the offshore direction can be predicted. This is because such features will either be at the standing infragravity wave nodes or antinodes when the mode of sediment movement is by bedload or suspended load, respectively. The distance (x) from the shoreline to consecutive nodes of the standing wave is given by;

$$x = \frac{g T_e^2 \tan \beta \chi}{4\pi^2} \quad (21) \text{ (Bowen, 1980)}$$

where:

1.  $T_e$  is the period of the standing infragravity wave
2.  $\chi$  is the non-dimensional distance from the shoreline to a given node or antinode and is given in Table#2.

Table#2 Non-dimensional distance from the shoreline to nodes of infragravity waves. Taken from Short (1999).

Wave Type	Node 1	Node 2	Node 3	Node 4	Node 5
Edge Wave Mode1	1.5				
Edge Wave Mode2	1.5	8.5			
Edge Wave Mode3	1.5	8.0	22.0		
Edge Wave Mode4	1.5	7.9	20.4	42.3	
Edge Wave Mode5	1.4	7.8	19.8	39.0	69.5
Leaky Wave	1.4	6.6	17.6	33.8	54.8
	Antinode 1	Antinode 2	Antinode 3	Antinode 4	Antinode 5
Edge Wave Mode1	4.5				
Edge Wave Mode2	3.9	16.1			
Edge Wave Mode3	3.8	13.6	35.1		
Edge Wave Mode4	3.7	13.0	29.6	61.6	
Edge Wave Mode5	3.7	12.8	28.1	52.2	95.7
Leaky Wave	3.5	12.3	25.8	44.5	67.8

For standing edge waves in the longshore direction the continuation of any longshore bars will be terminated by the formation of rip channels. The location of such channels, although being at the nodes of the longshore standing edge wave, cannot be predicted. However, the distance between them can be calculated as it is half the wavelength of the edge waves and can be obtained from the following formula.

$$\frac{\lambda_e}{2} = \frac{g}{4\pi} T_e^2 (2n+1) \tan \beta \quad (22) \text{ (Short, 1999)}$$

where:

1.  $\lambda_e$  is the edge wave length.
2.  $n$  is the mode number of the edge wave.

This equation however, can be simplified for steep reflective beaches ( $\tan\beta > 0.01$ ). This is because for such beaches, Guza and Davis (1974) made the observation that mode 0 subharmonic edge waves (edge waves having half the period of the incident waves) predominate with smaller synchronous edge waves (edge waves having the same period as the incident waves) also having a tendency to dominate on such beaches. Using these observations the distance between rip channels dissecting any longshore bar can be simplified to the following equations:

$$\frac{\lambda_e}{2} = \frac{g}{\pi} T_i^2 \tan\beta \quad (23a) \text{ subharmonic edge waves}$$

$$\frac{\lambda_e}{2} = \frac{g}{2\pi} T_i^2 \tan\beta \quad (23b) \text{ synchronous edge waves}$$

In the above paragraphs regarding predicting which beaches will have bars formed by cross-shore standing infragravity waves, how many will form and their associated offshore crest positions, it is assumed in the models that there is a dominant infragravity frequency. This assumption however is rarely valid with the infragravity energy spectrum being broad banded and often with no dominant modes. Only in storm conditions when the surf zones are wider has dominant infragravity modes been observed in the surf zone (Short and Aagaard, 1991). Even with this assumption not being valid most of the time however, Short and Aagaard found that the ability of  $B_*$  to predict the number of likely bars was surprisingly good (Ibid).

For single longshore bars which have formed as a result of the convergence of the onshore wave induced movement of sand with the offshore movement caused by plunging waves breaking Holman and Sallenger (1993) have constructed a model which predicts the location of the bar crest at  $x_{\text{bar}}$  meters from the shoreline with  $x_{\text{bar}}$  taking the following form:

$$x_{\text{bar}} = \frac{h_{\text{bar}}}{\tan\beta} = \frac{\gamma H_b}{\tan\beta} \quad (24)$$

where:

1.  $h_{\text{bar}}$  is the depth where the waves break.
2.  $H_b$  is the wave breaker height.
3.  $\gamma$  is a constant of order 1 and expresses the empirical ratio of wave height to depth of breaking waves. Thus wave height provides the primary scaling for bar distance.

One drawback of the above model is that waves are rarely monochromatic but instead have a spectrum of wave heights. Thus instead of monochromatic waves breaking at a single point and generating a sand bar, normal waves break over a region and it is unclear if a bar will form by this mechanism or if one will form where it will be located. However, it is known that once a bar forms, it does have the ability to focus wave energy which allows it to

grow further through positive feedback (Holman and Sallenger, 1993). Similar positive feedback mechanisms have been observed between pre-existing multiple bars and cross-shore standing edge waves (Ibid).

The slope of the beachface or swash zone is determined from the balance between two factors; the strength of the swash, which results in onshore sediment movement, and gravity which results in offshore sediment movement. The region over which the beachface slope is defined is within the mid-intertidal zone with the beachface slope normally being concave in the seaward direction and rarely being planar. For a net offshore sediment movement the beachface slope becomes flatter, whilst the beachface becomes steeper when there is a net onshore movement of sediment.

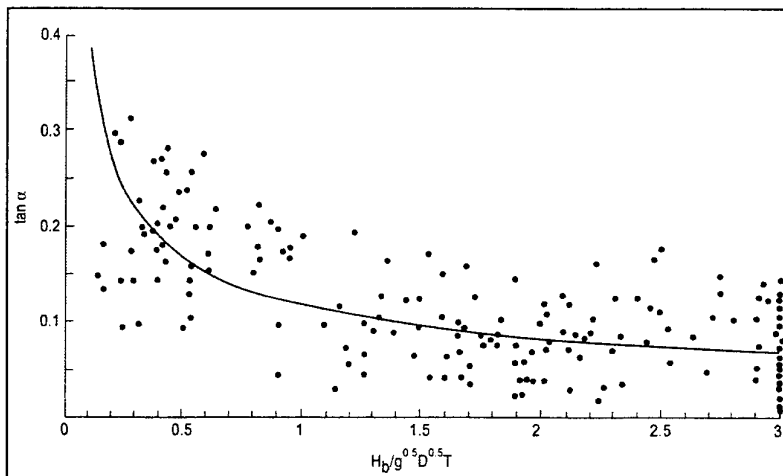
Sunamura (1984b) using the results from over 35 publications in conjunction with dimensional analysis derived the following empirical formula for the equilibrium beach face slope in unsaturated conditions.

$$\beta = \frac{0.12}{\sqrt{(H_b T \sqrt{gd_{50}})}} \quad (25)$$

where:

1.  $\beta$  is the beach face slope in degrees.

In obtaining this relationship it was observed that there was a lot of scatter of the data about this function. Figure#24 shows this function and the data it was obtained from. From this observation it was concluded that there were other factors not considered in equation #25 which have an influence of the slope of the beach face.



Figure#24 Data points generated when the measured beachface slope is plotted against the dimensionless parameter  $\left( \frac{H_b}{T \sqrt{gD}} \right)$ . The least square fit is also shown. From Short (1999).

One parameter which can have an influence on the slope of the beach face is the level of the water table at the beachface or the water content of the beachface sediment. Such a factor is

particularly important on macro-tidal beaches where two different intertidal profiles can exist. In an effort to extend the work of Sunamura to include saturated beaches, Turner (1994) investigated 15 macro-tidal beaches in Queensland, Australia where there were lower parts of the beachface that were permanently saturated. By re-analysing the work of Sunamura, Kriebel, Kraus and Larson (1991) derived the following relationship (equation#26) for the equilibrium slope of saturated beachfaces. It should be noted however, that, in comparison to the number of data points used to derive the unsaturated beachface slope, only a limited number were used to derive the following equation.

$$\beta = 0.05 \sqrt{\left( \frac{\omega_s T}{H_b} \right)} \quad (26)$$

where:

all parameters have been previously defined.

In order to utilise equation#26 the settling velocity would need to be either measured or calculated. Section#3.4 outlines the way the ADF could calculate this value.

### 6.1.1 Summary

Currently it is possible to predict the number of longshore bars that exist along any beach, the location of the crests in the offshore direction, and the beachface slope for saturated and unsaturated beachfaces. It is not possible to use numerical models to predict the longshore and cross-shore two dimensional morphology within the surf zone at any point in time. Such information must be collected using instruments such as Laser Airborne Depth Sounders.

### 6.1.2 Recommendations

From analysing the constituents of the above models and comparing them to what the ADF is likely to be able to measure or predict, it is foreseen that it would be possible for the ADF to use the Bar Parameter ( $B_*$ ) to predict which beaches will have bars forming by cross-shore standing infragravity waves and approximately how many are likely to form. The offshore position of the bar crests formed by infragravity waves as well as the longshore rip channels formed by the presence of edge waves, however, cannot be predicted as the dominant infragravity wave period needs to be known and such a parameter cannot be predicted and is very difficult to measure.

For single longshore bars which have formed by monochromatic breaking waves, the model which describes the offshore location of the bars crests (equation#24) should be viable to use by the ADF, as it is only requires very basic input parameters.

The models described above for predicting the slope of the beachface under saturated and non-saturated conditions, can be used by the ADF, although the model for saturated beachfaces requires that a small sediment sample be obtained and the median grain size visually estimated.

## 6.2 Temporal Evolution Models

### 6.2.1 Introduction

Broadly speaking, there are three types of morphological models which predict how different aspects of the surf zone morphology change in time. These include beach planshape models, coastal profile models, and coastal area models (Soulsby, 1997). The beach planshape models predict the evolution of the shape of the shoreline (for example the still water level). They achieve this by first calculating longshore transports at equally spaced points along a shore and by then applying the sediment budget. These types of models, however, work over time scales of years and decades. Hence, they are not relevant from the point of view of nearshore modelling for supporting amphibious operations. The other two types of models are relevant to the support of amphibious operations and are explained in the following paragraphs.

### 6.2.2 Coastal Profile Models

Coastal profile models are only concerned with how the cross-shore beach profile (or topography) evolves in time due to varying environmental forces. These types of models are more computationally demanding than beach planshape models and as such can only be applied to smaller time scales (typically several weeks or months). This type of modelling can be achieved by numerous methods and include: (1) Descriptive models, (2) Equilibrium models, (3) Empirical models, and (4) Process based models, (Roelvink and Broker (1993).

Descriptive models are useful in predicting the typical topography expected at any beach as well as transitions between different beach states. Such predictions are achieved by using governing parameters as indicators, with such parameters determined from beach observations obtained over as long a period as possible (preferably several months or more). A common governing parameter is Dean's (1973) parameter  $\Omega$  (Dean, 1991; Roelvink and Broker, 1993; Short, 1999), which was called the dimensionless fall velocity in section 3.4 (see Eqn.#9). This parameter is based on the observation that wave dominated beaches can be classified using wave height ( $H_b$ ), wave period ( $T$ ) and grain size (as defined by the sediment fall velocity  $\omega_s$ ) (Short, 1999). Descriptive models, however, cannot be used to infer beach changes caused by man made (or proposed man-made) structures. They also have limited quantitative capabilities (Roelvink and Broker, 1993).

Dean's parameter 
$$\Omega = \frac{H_b}{\omega_s T} \quad (27)$$

Equilibrium profile models are basic algebraical models which predict the new cross-shore beach profile that would occur if all environmental forces were in equilibrium (which would be when rate of sedimentation equals the rate of erosion). Equilibrium profile models are useful in cases of sandy beaches where longshore sand transport rates are negligible and can be used for establishing equilibrium profiles at time scales from those of long storms to years.

One of the most widely used equilibrium profile models is that by Dean (1977) (as cited by Roelvink and Broker, 1993). This model describes the equilibrium cross-shore profile for

monotonic profiles that would occur because of a rise in sea-level due to such influences as storms. The model is a 2/3 power shape law with a constant of proportionality (A) that is dependent upon the sediment distribution (see Eqn.#28). Like equilibrium models in general, it assumes that there is no gradient in the longshore sand transport. Unfortunately, this model does not account for variations in the wave conditions, wind speeds or currents associated with varying sea levels.

Dean's Rule 
$$Z = AX^{2/3} \quad (28)$$

Where

1.  $z$  and  $x$  represent the vertical and offshore axis, respectively.
2.  $A$  is a scale factor which is primarily dependent upon sediment characteristics.

Empirical profile evolution models illustrate the evolution of the cross-shore beach topography towards its equilibrium profile and are basic numerical models in the sense that they have empirically derived constants and relationships. These models can be applied to monotonic beach profiles as well as beaches with longshore bars and troughs, and have an important application of evaluating damage caused by storms of limited duration (Roelvink and Broker, 1993). One of the disadvantages of these types of models is that empirical coefficients must be determined for each beach.

Process-based models are models which have a module for each process which contributes to the morphological changes. The modules can be for tides, waves, nearshore velocities, cross-shore sediment transport and morphology, with the morphological modules normally based upon solving the sediment budget equation for bed height ( $z_b$ ). The sediment budget equation for non-horizontal beds is given by the following equation (taken from de Vriend *et-al.*, 1993).

$$\left( (1 - \epsilon_p) \frac{\partial z_b}{\partial t} + \frac{|q_t|}{h} \left( b_1 \frac{\partial z_b}{\partial s} + b_2 \frac{h}{R_n} \right) - \beta \left[ \frac{1}{l_n} \frac{\partial}{\partial s} \left( |q_t| \frac{\partial z_b}{\partial s} \right) + \frac{1}{l_s} \frac{\partial}{\partial n} \left( |q_t| l_s \frac{\partial z_b}{\partial n} \right) \right] \right) = 0 \quad (28)$$

where:

1.  $t$  is time (sec),
2.  $\epsilon_p$  is the bed porosity (dimensionless),
3.  $s$  and  $n$  are the distance along and orthogonal to streamlines (m),
4.  $q_t^1$  is the total sediment transport for a horizontal bed,
5.  $b_1$  and  $b_2$  are constants,
6.  $h$  is the water depth (m),
7.  $R_n$  is the radius of curvature of the streamlines,
8.  $l_s$  and  $l_n$  are metric coefficients related to the curvilinear coordinate system,
9.  $\beta$  is the downslope (gravitational) sediment transport.

Process based models are computer extensive models and have the major disadvantage that they require knowledge of the nearshore sediment characteristics to be applied. They also

have the disadvantage that they should only be applied by personnel with a strong background in nearshore modelling.

#### 6.2.3 Coastal Area Models

These two dimensional (area) morphology models are essentially the same as the process-based models, with the only difference being that the longshore sediment transport as well as the cross-shore transport are included in solving the sediment budget equation for bed depth. These types of models have individual modules (or numerical models) for waves, currents and sediments and in the long term are thought to be the best way to model all aspects of the nearshore environment. However, they are computer resource expensive models, can cost a large amount of money (> \$100K AUS) and need to be adjusted for each application by experienced personnel. They are normally purchased as whole packages with associated software from such organisations as HR Wallingford, Wallingford, UK; and Delft Hydraulics, Netherlands.

#### 6.2.4 Summary

From reading the literature it has been observed that there are three types of morphological models which predict how the morphology of the surf changes in time. These include, beach planshape models, coastal profile models and coastal area models (Soulsby, 1997). Although coastal profile models and coastal area models were deemed useful in the planning of amphibious operations, beach planshape models, were not. This is because such models predict the evolution of the shape of the shoreline over time scales of years and decades.

#### 6.2.5 Recommendations

By comparing the complexity of the temporal morphology models described above against the *in-situ* parameters the ADF would need to measure to use them, it was quickly concluded that the ADF was not in a position to use such models.

## 7. Summary

Before summarising the models found within the scientific literature that were deemed viable for the ADF, it should be stated that in numerous cases the best predictive models could not be recommended because they were either too complicated or required input parameters which were too difficult to acquire. Hence a subliminal lesson from the work conducted here, is that there can sometimes be a large difference between what is available from the scientific community as a result of research and what can be viably implemented from an operational perspective.

Keeping the above paragraph in mind, it was concluded that the most useful model for calculating the longshore velocity within the surf zone as a result of breaking waves was that developed by Komar and Inman (1970). Such a model is only applicable to monotonically sloping beaches of constant slope and for monochromatic waves, is not as accurate as more complicated models although was recommended because it has the large benefit of only requiring wave characteristics as input.

Currently there are no numerical models in existence which permit the longshore and offshore currents in the surf zone, generated by gradients in radiation stress, to be predicted as a function of time and space. Such models would require a large number of parameters as input and it is thought that such models will not be available for at least 5 years. What has been found are the range in velocity strengths of rips and mean values in longshore spacing of rips. A quantitative model developed by Martens *et-al.* was also found which permits the ability of topographic rips to form in embayments to be predicted.

Models for forecasting of the sediment concentration in the vertical (which is very helpful in forecasting the horizontal visibility range) due to the action of currents, unbroken and broken waves were outlined in the text. However, it was quickly concluded that due to such models requiring complex parameters as input none could be recommended to the ADF.

For predicting nearshore morphology characteristics it was found that there are no numerical models in existence which permit such characteristics to be predicted in the longshore and offshore direction. Such information would need to be gathered from high resolution instruments as Laser Airborne Depth Sounders. What was found were models that allowed the characteristics of longshore bars to be predicted. In particular it was concluded that it would be possible for the ADF to use the Bar Parameter ( $B_s$ ) to predict which beaches will have bars forming by cross-shore standing infragravity waves and approximately how many are likely to form. Models describing the offshore position of the bar crests formed by standing infragravity waves as well as the separation distance of longshore rip channels were also identified, however, they could not be recommended to the ADF as the dominant infragravity wave period needed by them cannot be predicted and is difficult to measure.

For single longshore bars which have formed by breaking waves, the model which describes the offshore location of the bars crests (equation#24) should be viable to use as it is only requires basic input parameters. Lastly, models enabling the slope of the beachface to be predicted for saturated and non-saturated conditions were also found (equations#25 and#26) and they too can be recommended to the ADF, but only if a small sediment sample is obtained and the median grain size estimated.

Finally numerical models were identified within the literature which enable the temporal changes that occur to nearshore morphology from time scales of days to years to be predicted. Such models however were foreseen as not viably useful to the ADF because they require *in-situ* data which would be difficult to obtain.

## 8. Summary Table

Longshore velocity strength on beaches with no rip cells.

Reference	Assumptions	Input Parameters
Komar and Inman (1970)	Plane beaches with monochromatic waves	Breaking wave height, wave propagating angles

Thornton and Guza (1986)	Plane beaches with irregular waves, wave length to depth ratio $<1/20$	Wave propagating angles, wave type, water depth, surf zone slope, deep water wave height, peak wave frequency, coastline orientation.
Smith, Larson and Krauss (1993)	Non-monotonic beaches with monochromatic waves.	Breaking wave height, propagation angle, wave period.

Longshore velocity with offshore velocity (two dimensional models)

Prognostic Parameter	Reference	Input Parameters
Longshore spacing between edge wave induced rips	Short (1999)	Edge wave period, edge wave node, surf zone slope
Longshore velocity variation in the longshore direction in the trough separating a bar (dissected by rip channels) and the swash zone.	Dalrymple (1978)	Cross-sectional area of trough, offshore wave steepness, depth over bar
Mega Rip formation	Martens, Williams and Cowell (1999)	Embayment Dimensional Characteristics, breaking wave height, wave period and sediment settling velocity.

Vertical distribution of suspended sediment.

Forcing Parameter	Reference	Input Parameters
Horizontal currents	Van Rijn	Water depth, water density, sediment reference concentration, vertical stress, sediment settling velocity.
Horizontal currents with unbroken waves	Souslby (1997)	Mostly the same as the above parameters.
Broken waves in the inner surf zone	Fredsoe and Deigaard (1992)	Mostly the same as the above parameters.

Morphology Characteristics (spatially indicative models)

Prognostic Parameter	Reference	Input Parameters
Offshore location of single sand bars formed by the action of breaking waves.	Hollman and Sallenger (1993)	Wave height at breaking and bed slope.

Bar Parameter ( $B_s$ ) [if bars will form by reflected infragravity waves, and if so how many].	(Short and Aagaard (1993)	Incident wave period, surf zone bed slope, distance from shoreline where monotonic slope terminates.
Offshore location of sand bars formed due to standing infragravity waves	Bowen (1980)	Infragravity wave period, surf zone bed slope.
Longshore Spacing between rip channels.	Short (1999)	Edge wave period, edge wave node and surf zone slope.
Beach face slope	Sunamura (1984b)	Wave height at breaking, wave period and median grain size.

#### Morphology Characteristics (Temporally indicative Models)

Type of Model	Reference	Input Parameters
Coastal Profile Models	Dean (1977)	Breaking wave height, wave period and sediment settling velocity
Coastal Area Models		Incident wave characteristics, surf zone sediment characteristics, surf zone bathymetry and tidal characteristics.

## 9. Acknowledgments

First and foremost I would like to thank my Task Manager Dr Phil Mulhearn and the librarians at DSTO Pyrmont for making available to me many helpful books and journal articles. I would also like to thank Associate Professor Andy Short (University of Sydney) for providing helpful advice.

## 10. Bibliography

Andrew, C.J.F. (1999) Bibliographic Review of Nearshore Wave Models. DSTO General-Document 0214.

Bailard, J.A. (1981) An "energetics" total load sediment transport model for a plane sloping beach. *J. Geophys. Res.* 86 (C11). 10938-54.

Bearman, G. (1989) Waves, Tides and Shallow-water processes. Pergamon. Oxford. 187pp.

Bowen, A.J. (1969) The generation of longshore currents on a plane beach. *J.Mar.Res.* 27: 206-215.

Bowen, A.J. (1980) Simple models of nearshore sedimentation; beach profiles and longshore bars. In McCann S B (Ed). The Coastline of Canada. Geological Survey of Canada, Paper 80-10, 1-11.

Bruun, P (1954) Coast erosion and the development of beach profiles. U.S. Army Beach Erosion Board Tech. Memo. #44

Dalrymple, R.A. (1978) Rip currents and their causes. Proceedings of the 16th Coastal Engineering Conference, Hamburg, 2:1414-1427.

de Vriend, H.J., Zyberman, J., Nicholson, J., Roelvink, J.A., Pechon, P. and H.N. Southgate (1993) Medium-term 2DH coastal area modelling. *Coastal Eng* 21:193-224.

Dean, R.G. (1977) Equilibrium beach profiles: U.S. Atlantic and Gulf Coasts. Tech. Rep. No. 12, University of Delaware, Newark.

Dean, R.G. (1991) Equilibrium beach profiles: characteristics and applications. *J. Coastal Res.* 7:53-84.

Deigaard, R.(1998) Comparison between a detailed deterministic sediment transport model and the Bailard formula. Proc. Coastal Dynamics '97 Conf.

Deigaard, R., Fredsoe, J. and Hedegaard, I.B.(1986) Suspended sediment in the surfzone. *J. Waterway, Port, Coastal and Ocean Eng.*, ASCE, 112(3): 351-369.

Del Balzo, D., Vodola, P. and Beveridge, J (1999) Environmental Factors in Amphibious Operations, *Military Operations Research*, Volume#4, pp 63-75.

Eagleson, P.S. (1965) Theoretical study of longshore currents on a planar beach. M.I.T. Hydrodynamics Laboratory. Tech.Rep.82:1-31.

Fredsoe, J. and R. Deigaard (1992) Mechanics of coastal sediment transport. World Scientific. Singapore. pp 369.

Gallagher, B. (1971) Generation of surf beat by non-linear wave to wave interactions. *J.Fluid.Mechanics.* 49:1-20.

Galvin, C.J. (1967) Longshore Current velocity: A review of theory and data. *Rev. Geophys.* 5: 287-304.

Galvin, C.J. and P.S. Eagleson (1965) Experimental Study of Longshore Currents on a Plane Beach. U.S. Army Corps Engr., CERC Technical Memo No.10.

Garcia, M. and Parker, G. (1991) Entrainment of bed sediment into suspension. *J.Hydr.Div.Proc. ASCE*, 117(4) 414-35.

Gourlay, M.R. (1968) Beach and Dune Erosion Tests, Delft Hydraulics Laboratory, Report No. M935/M936.

Grass, A.J. (1981) Sediment transport by waves and currents. Rep FL 29, SERC London Cent. Mar.Tech., London, UK.

Hallermeier, R.J. (1981) Terminal settling velocity of commonly occurring sand grains. *Sedimentology*, 28:859-865.

Harris, P.T (1994) Comparison of tropical, carbonate and temperate, siliciclastic tidally dominated sedimentary deposits: Examples from the Australian continental shelf. *Aust. J. Earth. Sciences.* 41:241-254.

Holman, R.A. (1995) Nearshore Processes. *Rev. Geophys.* Vol. 33 Suppl.

Holman, R.A. and Bowen, A.J. (1982) Bars, bumps and holes: Models for the generation of complex beach topography. *J.Geophys.Res.* 87:457-468.

Holman, R.A. and Sallenger, A.H. (1993) Setup and swash on a natural beach. *J.Geophys.Res.* 90:945-953.

Horikawa, K (1988) Nearshore dynamics and coastal processes: Theory, Measurement and Predictive Models. Univ. Tokyo Press. 422 pp.

Inman, D.L. and Quin, W.H. (1952) Currents in the surf zone. Proceedings of the 2<sup>nd</sup> Conf. of Coastal Eng. Council of Wave Research. 24-36pp.

Komar, P.D. (1976) Beach Processes and Sedimentation. Prentice-Hall, Englewood Cliffs, N.J. 429pp.

Komar, P.D. (1983) Handbook of coastal processes and erosion. CRC Press. Boca Raton, Florida.

Komar, P.D. (1998) Beach Processes and Sedimentation, 2<sup>nd</sup> Ed. Prentice Hall. Upper Sadle River, New Jersey.

Komar, P.D. and Inman, D.L. (1970) Longshore sand transport on beaches. *J.Geophys. Res.* 75: 5914-5927.

Komar, P.D. and Oltman-Shay, J. (1990) Nearshore currents. In: Handbook of Coastal and Ocean Engineering. Ed: Herbich, J. Gulf Publishing, Houston, Texas.

Kriebel, D.L., Kraus, N.C. and Larson, M (1991) Engineering methods for predicting beach profile response. *Coastal Sediments '91*. ASCE New York. 557-571.

Larson, M. and N.C. Kraus (1991) Numerical model of longshore current over bar and trough beaches. *J. Waterway, Port Coastal Ocean Eng.* 117(4) 326-347.

List, J.H. (1992) A model for the generation of two dimensional surf beat. *J. Geophys. Res.* 97: 5623-5635.

Longuet-Higgins, M.S. (1970a) Longshore currents generated by obliquely incident sea waves, 1. *J. Geophys. Res.* 75(33) 6778- 6789.

Longuet-Higgins, M.S. (1970b) Longshore currents generated by obliquely incident sea waves, 2, *J. Geophys. Res.* 75(33) 6790-6801.

Longuet-Higgins, M.S. and R.W. Stewart (1964) Radiation stresses in water waves- A physical discussion with applications, *Deep-Sea Res.* Vol 11. pp 529-562.

Martens, D., Williams, T. and Cowell, P.J. (in press) Mega-rip dimensional analysis on the Sydney coast, Australia and implications for beach state recognition and prediction. *J. Coastal Res.*

Nielsen, P. (1992) Coastal Bottom Boundary Layers and Sediment Transport. World Scientific Publishing, Singapore. Advanced Series on Ocean Engineering Vol 14.

Oltman-Shay, J (1998) Waves and Currents on a Washington Beach. Presentation at the American Geophysical Union Meeting in San Francisco, California.

Putnam, J.A., W.H. Munk and M.A. Taylor (1949) The prediction of longshore currents. *Trans. Am. Geophys. Union.* 30: 337-345.

Roelvink, J.A. and I. Broker (1993) Cross-shore profile models. *Coastal Eng.* 21: 163-191

Schoonees, J.S. (1996) Improvement of the most accurate longshore transport formula. Proc. ICCE 1996, Orlando, pp 3652-3665. ASCE.

Shemdin, O.H., K. Hasselman, S.V. Hsiao and K. Herterich (1978) Non-linear and linear bottom interaction effects in shallow water. Turbulence Fluxes Through the sea surface, Wave dynamics and Prediction. Eds. Favre, A. and Hasselman, K.. Plenum, 347-372 pp.

Short, A.D. (1999) Beach and Shoreface Morphodynamics. Lecture Notes. Sydney Uni.

Short, A.D. (Ed) (1999) Handbook of Beach and Shoreface Morphodynamics. Wiley and Sons, Great Britain.

Short, A.D. and Aagaard, T. (1993) Single and multibar beach change models. *J. Coastal Res.* Special Issue 15:141-157.

Smith, J.M. Larson, M. and Kraus, N.C. (1993). Longshore current on a barred beach: field measurements and calculation. *J. geophys. Res.* 98(C12) 22717-22,731

Smith, J.D. and McLean, S.R. (1977) Spatially averaged flow over a wavy surface. *J. Geophys. Res.* 82(12):1735-46.

Soulsby, R. (1997) Dynamics of marine sands. Thomas Telford . London. pp 249.

Sunamura, T. (1984b) Quantitative prediction of beachface slopes. *Geological Society of American Bulletin*. 95:242-245.

Thornton, E.B. (1970) Variation of longshore current across the surf zone. Proc. 12<sup>th</sup> Int. Coastal Engineering Conf. New York. Amer. Soc. Civil Eng., 291-308.

Thornton, E.B. and R.T. Guza (1983) Transformation of wave height distribution. *J. Geophys. Res.*, 88:5925-5938.

Thornton, E.B. and R.T. Guza (1986) Surf zone longshore currents and random waves: field data and models. *J. Physical. Ocean.* 16: 1165-1178.

Turner, I.L. (1994) Water table outcropping on macro-tidal beaches and its influences on morphology of the inter-tidal profile. Unpublished PhD thesis, Coastal Studies Unit, University of Sydney, 288pp.

Van Rijn, L.C. (1984) Sediment transport: Part I: bed load transport; part II: suspended load transport; part III: bed forms and alluvial roughness. *J. Hydraulic. Div.*, Proc. ASCE, 110 (HY10), 1431-56; (HY1), 1613-41; (HY12), 1733-54

Van Rijn, L.C. (1998) Principles of Coastal Morphology. Aqua Publications, Amsterdam, The Netherlands.

Wright, L.D. and Short, A.D. (1984) Morphodynamic variability of beaches and surf zones, a synthesis. *Marine Geology*, 56: 92-118.

## 11. Pertinent Literature

In determining which numerical models were currently available from the scientific community as well as conducting background reading, a number of key text books were identified. It was considered helpful for any future re-analysis of the topics listed in this GD if such text books were listed. These text books are as listed below.

Horikawa, K (1988) Nearshore dynamics and coastal processes: Theory, Measurement and Predictive Models. Univ. Tokyo Press. 422 pp.

Komar, P.D. (1983) Handbook of coastal processes and erosion. CRC Press. Boca Raton, Florida.

Komar, P.D. (1998) Beach Processes and Sedimentation, 2<sup>nd</sup> Ed. Prentice Hall. Upper Sadle River, New Jersey.

Short, A.D. (Ed) (1999) Handbook of Beach and Shoreface Morphodynamics. Wiley and Sons, Great Britain.

Soulsby, R. (1997) Dynamics of marine sands. Thomas Telford . London. Pp 249.

## DISTRIBUTION LIST

Reviewing Nearshore Current, Turbidity and Morphology Models

Colin J.F. Andrew

### AUSTRALIA

#### DEFENCE ORGANISATION

##### Task Sponsor

COMAUSNAVAMPHIBASGRP

##### S&T Program

Chief Defence Scientist  
FAS Science Policy  
AS Science Corporate Management  
Director General Science Policy Development  
Counsellor Defence Science, London (Doc Data Sheet)  
Counsellor Defence Science, Washington (Doc Data Sheet)  
Scientific Adviser to MRDC Thailand (Doc Data Sheet)  
Scientific Adviser Joint  
Navy Scientific Adviser  
Scientific Adviser - Army (Doc Data Sheet and distribution list only)  
Air Force Scientific Adviser  
Director Trials

} shared copy

##### Aeronautical and Maritime Research Laboratory

Director: Dr W. Schofield  
Chief of Maritime Operations Division: Dr N. Nandagopal  
Research Leader: Dr A. Theobald  
Group Head: Dr D. Cato  
Task Manager: Dr P. Mulhearn  
Author: Mr C. Andrew, MOD  
Mr Les Hamilton, MOD, Sydney  
Mr Jamie Watson, MOD, Sydney

##### DSTO Library and Archives

Library Fishermans Bend (Doc Data Sheet)  
Library Maribyrnong (Doc Data Sheet)  
Library Edinburgh  
Australian Archives  
Library, MOD, HMAS Stirling  
Library, MOD, Pyrmont 2 copies  
US Defense Technical Information Center, 2 copies  
UK Defence Research Information Centre, 2 copies

Canada Defence Scientific Information Service, 1 copy  
NZ Defence Information Centre, 1 copy  
National Library of Australia, 1 copy

#### **Capability Development Division**

Director General Maritime Development (Doc Data Sheet only)  
Staff Officer Amphibious and Afloat Support  
Land Development Branch-Staff Officer Amphibious Mobility  
Director General Aerospace Development (Doc Data Sheet Only)

#### **Knowledge Staff**

Director General Command, Control, Communications and Computers (DGC4) (Doc Data Sheet only)

#### **Navy**

SO (Science), Director of Naval Warfare, Maritime Headquarters Annex, Garden Island, NSW 2000. (Doc Data Sheet only)  
Director of Oceanography and Meteorology, Garden Island, NSW, 2000  
Officer in Charge, Australian Oceanographic Centre, Garden Island, NSW, 2000

#### **Army**

Amphibious Beach Team, 10 FSB, Ross Island Barracks, Townsville  
Stuart Schnaars, ABCA Standardisation Officer, Tobruk Barracks, Puckapunyal, 3662 (4 copies)  
SO (Science), Deployable Joint Force Headquarters (DJFHQ) (L), MILPO Gallipoli Barracks, Enoggera QLD 4052 (Doc Data Sheet only)  
NPOC QWG Engineer NBCD Combat Development Wing, Tobruk Barracks, Puckapunyal, 3662 (Doc Data Sheet relating to NBCD matters only)  
Mr T. Duell, Army Technology & Engineering Agency

#### **Intelligence Program**

DGSTA Defence Intelligence Organisation  
Manager, Information Centre, Defence Intelligence Organisation

#### **Corporate Support Program**

Library Manager, DLS-Canberra

#### **UNIVERSITIES AND COLLEGES**

Australian Defence Force Academy  
Library  
Head of Aerospace and Mechanical Engineering  
Hargrave Library, Monash University (Doc Data Sheet only)  
Librarian, Flinders University

#### **OTHER ORGANISATIONS**

NASA (Canberra)  
AusInfo

## OUTSIDE AUSTRALIA

### ABSTRACTING AND INFORMATION ORGANISATIONS

Library, Chemical Abstracts Reference Service  
Engineering Societies Library, US  
Materials Information, Cambridge Scientific Abstracts, US  
Documents Librarian, The Center for Research Libraries, US

### INFORMATION EXCHANGE AGREEMENT PARTNERS

Acquisitions Unit, Science Reference and Information Service, UK  
Library - Exchange Desk, National Institute of Standards and Technology, US

SPARES (4 copies)

**Total number of copies:** 55

<b>DEFENCE SCIENCE AND TECHNOLOGY ORGANISATION DOCUMENT CONTROL DATA</b>		1. PRIVACY MARKING/CAVEAT (OF DOCUMENT)	
<b>2. TITLE</b> Reviewing Nearshore Current, Turbidity and Morphology Models		<b>3. SECURITY CLASSIFICATION (FOR UNCLASSIFIED REPORTS THAT ARE LIMITED RELEASE USE (L) NEXT TO DOCUMENT CLASSIFICATION)</b> Document (U) Title (U) Abstract (U)	
<b>4. AUTHOR(S)</b> Colin J.F. Andrew		<b>5. CORPORATE AUTHOR</b> Aeronautical and Maritime Research Laboratory 506 Lorimer St Fishermans Bend Victoria 3207 Australia	
<b>6a. DSTO NUMBER</b> DSTO-GD-0306	<b>6b. AR NUMBER</b> AR-012-071	<b>6c. TYPE OF REPORT</b> General Document	<b>7. DOCUMENT DATE</b> November 2001
<b>8. FILE NUMBER</b> 490/6/91	<b>9. TASK NUMBER</b> NAV 98/025	<b>10. TASK SPONSOR</b> COMAUUSAMPHIBAS GRP	<b>11. NO. OF PAGES</b> 52
<b>13. URL on the World Wide</b> <a href="http://www.dsto.defence.gov.au/corporate/reports/DSTO-GD-0306.pdf">http://www.dsto.defence.gov.au/corporate/reports/DSTO-GD-0306.pdf</a>		<b>14. RELEASE AUTHORITY</b> Chief, Maritime Operations Division	
<b>15. SECONDARY RELEASE STATEMENT OF THIS DOCUMENT</b> <i>Approved for public release</i>			
OVERSEAS ENQUIRIES OUTSIDE STATED LIMITATIONS SHOULD BE REFERRED THROUGH DOCUMENT EXCHANGE, PO BOX 1500, SALISBURY, SA 5108			
<b>16. DELIBERATE ANNOUNCEMENT</b> No Limitations			
<b>17. CASUAL ANNOUNCEMENT</b> Yes <b>18. DEFTEST DESCRIPTORS</b> Bibliography, littoral currents, sediment transport, water analysis, transparency, geomorphology			
<b>19. ABSTRACT</b> The aim of this investigation was to review the different types of nearshore current, turbidity, and morphology evolution models currently available and to recommend those most suitable for aiding the planning of amphibious operations. This was achieved by first reading relevant literature and listing the different types of models found within it. Then their relevant attributes (for example: the equations and assumptions utilised in developing them, the parameters needed to utilise them, any validation exercises performed, their findings and their accuracy) were analysed. An important observation made here was that some potentially useful numerical models could not be recommended for usage to the RAN as they required parameters which were too difficult to acquire.			

TECHNICAL REPORT DSTO-GD-0306 AR-012-071 NOVEMBER 2001